PRC2 enacts Wnt signaling in intestinal homeostasis and contributes to the instigation of stemness in diseases entailing epithelial hyperplasia or neoplasia

Short title: PRC2 balances intestinal stem cell differentiation

Mikko Oittinen[1], Alina Popp[1,2], Kalle Kurppa[1], Katri Lindfors[1], Markku Mäki[1], Minna U. Kaikkonen[3] and Keijo Viiri[1*]

[1]Tampere Centre for Child Health Research, University of Tampere and Tampere University Hospital, Tampere, Finland. [2]University of Medicine and Pharmacy "Carol Davila" and Institute for Mother and Child Care, Bucharest, Romania. [3]Department of Biotechnology and Molecular Medicine, A.I. Virtanen Institute for Molecular Sciences, University of Eastern Finland, Kuopio, Finland.

Author contributions

MO: Collection and assembly of data, data analysis and interpretation, manuscript writing and final approval of manuscript. AP: Provision of study material and patients and final approval of manuscript. KK: Financial support, provision of patients and final approval of manuscript. KL: Financial support, administrative support and final approval of manuscript. MM: Financial support, administrative support, provision of patients, and final approval of manuscript. MUK: Collection and assembly of data, data analysis and interpretation, manuscript writing and final approval of manuscript. KV: Conception and design, financial support, collection and assembly of data, data analysis and interpretation, manuscript writing and final approval of manuscript

[*]**Corresponding Author**: Keijo Viiri, PhD, University of Tampere, Biokatu 10, 33520, Tampere, Finland. E-mail: keijo.viiri@uta.fi, Tel: +358405549648

Disclosure: The authors have nothing to disclose

ACKNOWLEDGEMENTS

Funding: This work was supported by Academy of Finland (265575), Päivikki and Sakari Sohlberg Foundation, Sigrid Jusélius Foundation, Tekes – The Finnish Funding Agency for Innovation (658/31/2015) and Competitive State Research Financing of the Expert Responsibility Area of the Tampere University Hospital, Grant 9T040. M.U.K was supported by the Academy of Finland, Sigrid Jusélius Foundation, Finnish Foundation for Cardiovascular Research and Finnish Cultural Foundation. We thank The Sequencing Service GeneCore Sequencing Facility (EMBL, http://www.genecore.embl.de) for DNA sequencing.

Key words: Intestinal stem cells, Polycomb Repressive Complex 2 (PRC2), Wnt signaling, celiac disease, enterocyte, crypt hyperplasia

ABSTRACT

Canonical Wnt/β-catenin signaling regulates the homeostasis of intestinal epithelium by controlling the balance between intestinal stem cell self-renewal and differentiation but epigenetic mechanisms enacting the process are not known. We hypothesized that epigenetic regulator, Polycomb Repressive Complex-2 (PRC2), is involved in Wnt-mediated epithelial homeostasis on the crypt-villus axis and aberrancies therein are implicated both in celiac disease and in intestinal malignancies. We found that PRC2 establishes repressive crypt and villus specific H3K27me3 signature on genes responsible for e.g. nutrient transport and cell killing in crypts and e.g. proliferation and differentiation in mature villi, suggesting that PRC2 facilitates the Wnt-governed intestinal homeostasis. When celiac patients are on gluten-containing diet PRC2 is out-of-bounds active and consequently its target genes were found affected in intestinal epithelium. Significant set of effective intestinal PRC2 targets are also differentially expressed in colorectal adenoma and carcinomas. Our results suggest that PRC2 gives rise and maintains polar crypt and villus specific H3K27me3 signatures. As H3K27me3 is a mark enriched in developmentally important genes, identified intestinal PRC2 targets are possibly imperative drivers for enterocyte differentiation and intestinal stem cell maintenance downstream to Wnt-signaling. Our work also elucidate the mechanism sustaining the crypt hyperplasia in celiac disease and suggest that PRC2-dependent fostering of epithelial stemness is a common attribute in intestinal diseases in which epithelial hyperplasia or neoplasia prevails. Finally, this work demonstrates that in intestine PRC2 represses genes having both pro-stemness and pro-differentiation functions, fact need to be considered when designing epigenetic therapies including PRC2 as a drug target.

INTRODUCTION

Polycomb Group (PcG) proteins regulate developmental gene expression during cell differentiation. PcG proteins are essential for embryonic stem cell self-renewal and pluripotency but they are also necessary for the maintenance of cell identity and cell differentiation throughout life [1]. PcG proteins form at least two Polycomb Repressive Complexes (PRC). PRC2 catalyses trimethylation of histone H3 lysine 27 (H3K27me3), forming a binding site for PRC1 [2]. In embryonic stem cells PRC2 represses the expression of developmental regulators necessary for cell differentiation [3]. In differentiated cells, genes important for the given cell identity lose H3K27me3 whereas genes that regulate alternate cell-types remain methylated and repressed [4].

Perturbations in epigenetic mechanisms can contribute to diseases such as cancer. For instance, PcG protein EZH2 has been shown to be overexpressed in endometrial, prostate, breast, colon, lung and skin cancers [5]. It has been shown that overexpressed PcG proteins keep cells in more proliferative, low differentiation state that inevitably is one of the hallmarks of cancer. The crypt-villus axis constitutes a functional unit of the small intestine, where intestinal stem cells (ISC) and transit amplifying (TA), migrating and differentiating precursor epithelial cells are restricted to the crypts and mature absorptive epithelial cells are restricted to the villi. Epithelial cells undergo rapid turnover, and thus are tightly regulated to maintain homeostasis between proliferation, differentiation and apoptosis [6]. Reminiscent of hyper-proliferative state in cancer, the main manifestation of dietary gluten-induced celiac disease, is also the increased proliferative and lesser differentiation state, namely of the epithelium of the small intestine showing an enteropathy with crypt hyperplasia and villous atrophy [7].

Wnt-signaling genes are bound by PRC2 in human embryonic stem (ES) cells [8] and also in adult tissues e.g. in adipogenesis [9]. Canonical Wnt-signaling is essential for homeostasis of the healthy intestinal epithelium [10] but epigenetic factors running the errands of Wnt-signaling in

intestine are not known. Recently it has been proposed that intestinal stem cells as well as secretory and absorptive progenitor cells show comparable levels of histone modifications at most of the same cis-elements in the genome [11]. This work measured the levels of H3K4me2 and H3K27ac, whereas PRC2 activity (H3K27me3) was not investigated. Recently, it was shown that PRC1 activity is required for the integrity of the intestinal epithelium [12] but whether PRC2 is involved in the differentiation of the epithelium of the small intestine is not currently known. We pursued to understand this by using mouse mini-gut organoid cultures [13] and high-throughput-methods, such as ChIP-Seq and GRO-Seq to identify factors that contribute to the development of the small intestine. We found that PRC2 regulates substantial subset of genes, which in particular, have a function in development of the gut epithelium. Furthermore, we found that aberrant PRC2 activity is associated with celiac disease, and the PRC2 governed intestinal transcriptome is dysregulated in colorectal adenomas and cancers.

MATERIALS AND METHODS

Mini-gut organoid and cell line cultures

Mouse mini-gut organoids were grown essentially as described previously [13, 14]. To model intestinal crypt-villus axis organoids were grown in the presence of Wnt3A, EGF, Noggin, R-spondin and CHIR-99021 (WENRC stem cell media) and differentiation was induced by omitting Wnt3A and CHIR-99021 and media was supplemented with Wnt-inhibitor IWP-2 (ENRI enterocyte differentiation media). T84 cells were grown as previously [15] except we used Matrigel GFR instead of collagen.

Patient material

Altogether six stored formalin-fixed and paraffin-embedded small intestinal biopsy samples from adult celiac disease patients adhering to a strict gluten-free diet for at least two years and being in clinical remission were selected, as well as their biopsies after a 12-week gluten challenge [16]. The study

protocol was approved by the Ethics Committee of Tampere University Hospital, (Ethical permission R07129M). All subjects had given written informed consent.

ChIP-Seq analysis

Mini-gut organoids (in WENRC and ENRI culturing conditions) were isolated from Matrigel with Cell Recovery Solution (Corning, NY) followed by washes with cold PBS and brought to single cell suspension with TrypLE Express (Thermo Fisher Scientific, Waltham, MA) and counted. Equal number of cells were cross-linked with formaldehyde and nuclei were isolated, lysed, and sonicated with a Covaris S220 ultrasonicator. The resulting nuclear extract was incubated overnight at 4 °C with Dynal Protein G beads pre-incubated with 5µg of H3K27me3 or H3 (ab6002 and ab1791, respectively, Abcam, Cambridge, UK) antibody. Beads were washed and bound complexes eluted, and cross-links were reversed by heating to 65 °C. IP and input DNA were then purified by a treatment with RNAse A, proteinase K, and phenol:chloroform extraction. Libraries were constructed from IP and input DNA by NEBnext® Ultra™ DNA-library preparation kit for Illumina (NEB, Ipswich, MA) and subjected to 50 bp single-end read sequencing with Illumina Hiseq 2000 at EMBL Genecore, Heidelberg, Germany.

GRO-Seq analysis

Organoids were harvested (as in ChIP-Seq) and GRO-Seq was performed for equal number of isolated nuclei from WENRC and ENRI conditions grown organoids. The nuclei extraction and run on reaction was performed as described [17]. For each replicate, 3 million cells were suspended to a final volume of 80-200 µl of freezing buffer. The RNA was extracted using Trizol LS (Life Technologies, Carlsbad, CA), fragmented 13 mins in 70°C using RNA Fragmentation Reagents (Life Technologies) and purified by running through RNase-free P-30 column (Bio-Rad, Hercules, CA). The RNA was dephosphorylated with PNK for 2 hours (New England Biolabs, Ipswich, MA) followed by heat-

inactivation. Dephosphorylation reactions were purified using 65 µl of blocked (5x volume of 0.25xSSPE, 1 mM EDTA, 37.5 mM NaCl, 0.05% Tween-20, 0.1%PVP and 0.1% ultrapure BSA for 1hour in RT) anti-BrdU bead slurry (SantaCruz Biotech, Santa Cruz, CA) suspended in 500 µl of binding buffer (0.25xsSSPE, 1 mM EDTA, 37.5 mM NaCl 0.05% Tween-20). After binding for 1 h in RT, the beads were washed twice with binding buffer, twice with low salt buffer (0.2xSSPE, 1mM EDTA, 0.05% Tween-20) and once with high salt buffer (0.2xSSPE, 1mM EDTA, 135 mM NaCl0.05% Tween-20) and twice with TE-buffer (1xTE, 0.05% Tween-20). The RNA was eluted three times by using 130 µl of elution buffer (50 mM Tris-HCl pH 7.5, 150 mM NaCl, 0.1% SDS, 1mM EDTA and 20 mM DTT) followed by ethanol precipitation overnight. All buffers were supplemented with SUPERase In (2 µl/10ml; Life Technologies). The library preparation was performed the next day as described [18]. The libraries were amplified for 14 cycles and the final product of 190-350bp was extracted from on 10% Novex TBE gel (Life Technologies) and eluted from crushed gel slice twice using 100µl of elution buffer (TE+0.1% Tween+150 mM NaCl). The libraries were purified using ChIP DNA clean & Concentrator Kit (Zymo Research Corporation, Irvine, CA), quantified using the Qubit fluorometer and sequenced using Illumina HiSeq 2000 at EMBL Genecore, Heidelberg, Germany.

ChIP- and Gro-seq data analyses

Analyses were performed essentially as described in [17–19] (see Supplemental materials and methods for detailed descriptions of data analyses)

Immunohistochemistry

Formalin fixed paraffin embedded duodenal biopsies were cut to tissue sections and subjected to immunohistochemical staining using antibodies against Suz12 (Cell Signaling D39F6, 1:1600), Scin (Sigma-Aldrich HPA022009, 1:50) and SPHK1 (Sigma-Aldrich HPA028761, 1:100). Standard staining

procedures including heat induced epitope retrieval and quenching of endogenous peroxidase activity prior to antibody incubation were used. Patients on gluten free diet and gluten containing diet were compared (n=6) by evaluating the Suz12 staining. Length of the Suz12 positive area in 2-5 correctly aligned crypts was counted for each sample and reported as median.

Crude mechanical separation of mouse duodenal villi and crypts-TA fractions

Duodenal fragments were harvested from C57BL/6 mice and washed gently with cold PBS. Villus epithelium was released by pipetting fiercely up and down ten times in 15ml of cold PBS with 25ml pipette. PBS with released villus epithelium was collected and remaining epithelia in duodenal fragment was collected with 10ml washes of cold PBS two times and pooled with villus fraction. Remaining duodenal fragments were incubated in PBS-10mM EDTA at +4°C with gentle shaking. PBS-EDTA solution was removed and crypt-TA fraction was released by vigorously pipetting up and down thirty times in cold PBS followed by two subsequent washes with cold PBS.

Western blot for cells treated with EZH2 inhibitor

T84 cells and mouse organoids were treated with 5 μM of EZH2 methyltransferase inhibitor[20] for six days and cells were lysed in laemmli buffer, heated and ran to 15% SDS-PAGE gels and transferred to Hybond-C membrane (Amersham Biosciences, Bucks, UK). Decrease of bulk trimethylation of H3K27 was assessed with ab6002 antibody and compared to bulk amount of H3 ab1791 antibody (Abcam, Cambridge, UK)

Quantitative reverse transcription PCR (qRT-PCR)

RNA was extracted from cells/tissues using Trizol® (Invitrogen, CA) according to manufacturer's protocol. cDNA was synthesised with iScript™ cDNA synthesis kit, quantitative PCR reactions were performed with SsoFast™ EvaGreen® Supermix and reactions were run in CFX96 real-time PCR

detection systems (Bio-Rad laboratories, CA). List of qRT-PCR oligos used in this study are shown in Supplemental materials and methods.

RESULTS

PRC2 members are expressed in proliferating cells in intestinal crypts and regulate enterocyte differentiation

Research conducted using intestinal cancer-cell models have previously shown that disrupting PRC2 activity leads to a significant precocious expression of a number of terminal differentiation markers [21]. We also tested the effect of PRC2 inhibition by pharmacologically inhibiting the methyl transferase activity of EZH2 [20] in T84 cell intestinal differentiation model [15]. Inhibition of PRC2 activity significantly induced enterocyte differentiation (ALPI mRNA) with the concomitant decrease of the intestinal stem cell (ISC) marker LGR5 mRNA (figure 1A). Markers for paneth, enteroendocrine and goblet cells remained adamant, suggesting that PRC2 is governing only the enterocyte differentiation program in T84 cells. Next we sought to investigate whether PRC2 regulates enterocyte differentiation also in mouse mini-gut organoids [13, 22]. Inhibition of PRC2 activity, similarly as in T84 cells, induced significant and enterocyte specific differentiation with the concomitant decrease of ISC marker LGR5 (figure 1B).

To facilitate the study of PRC2 function in intestinal differentiation we optimized the mini-gut culture conditions to best recapitulate the composition of cell population along the crypt-villus axis. WENRC vs. ENRI (see methods) culturing conditions were best suited for this purpose as markers for crypt/ISC compartment were highly enriched; (LGR5 mRNA) 100-fold and paneth cells (LYZ mRNA) 14-fold, when mini-guts were cultured in WENRC compared to ENRI media.

Reciprocally, enterocytes (ALPI mRNA), enteroendocrine cells (CHGA mRNA) and goblet cells (MUC2 mRNA) were 50, 3 and 9 –fold upregulated in mini-guts grown in ENRI-media, respectively (Supplemental figure 1A-C). By immunohistochemical staining PRC2 has been shown to be expressed in transit amplifying zone (TA-zone) in the crypt where commitment to enterocyte differentiation is also taking place [21]. In addition to yielding composition of cell populations comparable to in vivo crypt and villus tip, also PRC2 members, SUZ12 and EZH2 were both ~5 to 7-fold less expressed in mini-guts differentiated with ENRI-media (figure 1C). We found this comparable with the *in vivo* expression of PRC2 members in crypt-villus-axis when measured from villus and crypt/ISCs+TA fractions isolated from mouse (figure 1D). Our data suggest that PRC2 regulates enterocyte differentiation *in vitro* and is expressed in intestinal crypt/TA-region and also demonstrates that the function of PRC2 in enterocyte differentiation can be studied in mini-gut organoid model.

PRC2 specify the crypt and villus domains in the small intestine

We next sought to determine the role of PRC2 in the epigenetic maintenance of ISCs and how epigenome is reprogrammed during the enterocyte differentiation process triggered by inhibition of Wnt-signaling. To this end, we performed ChIP-Seq for H3K27me3 antibody (and H3 as a control) in mini-guts grown in stem cell media (WENRC) and in enterocyte differentiation media (ENRI) (heat maps in Supplemental figure 2). We also gauged the gene expression levels by performing GRO-Seq experiments for the mini-guts grown in the same culturing conditions. We used GRO-Seq to capture nascent unspliced RNA production disclosing the real-time transcriptional status of any given locus thus allowing better comparison of the data to ChIP-Seq. We found 2610 differentially expressed genes when comparing mini-guts grown in WENRC and ENRI (Supplemental table I). Altogether 1185 genes were upregulated in mini-guts grown in WENRC and 1425 genes were upregulated when grown in

ENRI. When ChIP- and GRO-Seq data were combined we found that out of 2610 differentially expressed genes 90 were regulated by PRC2 (3.4 %). Gene expression heat map in figure 2A illustrates the genes differentially expressed in mature enterocytes and in crypt/ISC cells. Expression heat map in figure 2B depicts the expression for the 90 genes found to be regulated by PRC2. When composite enrichment profile of H3K27me3, across the TSS in genes that are silenced by PRC2 in crypts/ISCs, were constructed it became evident that in enterocytes these genes are demethylated and consequently activated (figure 2C). Figure 2D demonstrates the data for the reciprocally behaving genes i.e. genes active in ISCs and later silenced by PRC2 in mature enterocytes. Figure 2E further recapitulates the magnitude of genome-wide accumulation and erasure of H3K27me3 during the enterocyte differentiation and also shows that genes which are subject to highest resettling of H3K27me3 also show significant gene expression difference when measured by GRO-Seq. These results indicate that a subset of crypt and villus specific gene expression during the differentiation of the small intestinal epithelium is regulated by PRC2.

Novel intestinal PRC2 targets in mouse display villus and crypt specific expression pattern also in human tissues *in vivo.*

Next we surveyed whether crypt/villus gene expression pattern found in mouse mini-guts also exists in humans *in vivo*. Majority of the differentially expressed genes also show comparable expression gradient in crypt-villus axis in small intestine *in vivo* when they were searched in protein atlas database [23] whenever immunohistochemical staining of the given protein was available (Supplemental figure 3A-B). PRC2 was found to mark canonical intestinal stem cell gene LGR5 [24] and genes associated with stem cell functions e.g. ASCL2 [25], CD24a [26], Igfbp4 [27] and Tnfrsf19 [28] with H3K27me3 mark in mature enterocytes. Also negative regulator of Wnt-signaling gene, Axin2 [29], was found to

be a PRC2 target in villi (figure 3A). Figures 3B&C show some PRC2 targets and IHC staining snapshots from Protein Atlas database [23] providing confirmation that they are differentially expressed along the crypt-villus axis also *in vivo* in humans. We also tested the expression of the PRC2 targets silenced in mouse enterocytes by performing RT-qPCR from crude mechanically fractionated crypt+TA/ISC and villus compartments to show that crypt domain specific expression pattern is also taking place *in vivo* (figure 3D**).** All targets were enriched in crypt compartment in a statistically significant manner except Marcksl1 which has been shown to be expressed also in villous microfold-like cells (M-like cells) [30]. Crude mechanical fractioning was not applicable for enriching PRC2 targets silenced in crypts as we find that they were expressed in 1:1 villus:crypt –ratio, except Slc15a1 (6:1) (data not shown). Apparently crude mechanical villus fractioning detach only loose villus tip epithelium while terminally differentiated enterocytes in TA-region remain attached, as evinced by only subtle enrichment of Alpi (4-fold).

As PRC2 is known to preferably target genes having function in development and signaling, as seems to be the case also in the intestine (figure 3A), we believe that these novel PRC2 targets on crypt-villus axis are also imperative for intestinal homeostasis.

PRC2 determines the ISCs fate to enterocytes

In murine and human embryonic stem cells and cell types derived thereof, PRC2 targets developmental regulators that must be repressed to maintain cell identity [3, 31]. We therefore asked which kind of gene sets are silenced by PRC2 at both ends along the crypt-villus axis in the adult intestine. Analyses of the gene ontologies indicate that in crypt/ISC region PRC2 represses genes belonging to the functional categories quintessential to enterocyte functions such as transport of various small molecules

at the apical side of the cells and also genes positively contributing to cell killing. Of note, PRC2 seems to also regulate genes involved in actin mediated microvillus structures at the brush border (figure 4A). In the mature enterocytes, on the other hand, PRC2 represses genes participating in cell proliferation, differentiation, epithelium development and digestive tract morphogenesis. In addition, PRC2 is targeted to genes involved in cell adhesion, ontology closely linked to epithelium shedding in villus tip (figure 4B). Taken together, these gene ontology analyses indicate that PRC2 is significantly targeted to genes involved in variety of enterocyte specific molecular functions amid enterocyte differentiation.

Next we aimed to identify transcription factor target motifs enriched amongst PRC2 regulated genes. We found de novo motif with the best match to TCF3 binding site to be significantly enriched in PRC2 regulated genes ($P<10^{-12}$) when they were queried against PRC2-independent and differentially expressed genes along the crypt-villus axis (figure 4C**)**. In the context of embryonic stem cell maintenance and differentiation PRC2 is known to be preferably targeted to genes having CpG islands in their promoters [32]. We found that PRC2 inclines to target genes harboring CpG islands also along the crypt-villus axis since genes regulated independent of PRC2 have less CpG islands amongst them (figure 4D). For instance, 78% of the PRC2-dependent crypt and villus specific genes have a CpG island in their promoter whereas only 65% of the PRC2-independent crypt and villus specific genes have that. These analyses pertaining to PRC2 targets along the crypt-villus axis show that likewise in embryonic stem cell differentiation, PRC2 is preferably targeted to genes possessing CpG islands. Furthermore, homer de novo motif search data suggest that TCF3 transcription factor, as a known effector in Wnt/β-catenin signaling pathway [33] is possibly implicated in PRC2-dependent intestinal homeostasis.

PRC2 targets in intestine are implicated in colorectal adenomas and cancers

Next we sought to investigate how PRC2-regulated intestinal transcriptome is associated with colorectal neoplasias. The APC gene encodes an adenomatous polyposis coli tumor-suppressor protein, the germline mutation of which leads to familial adenomatous polyposis, an autosomal syndrome characterized by multiple colorectal lesions [34]. APC inactivation is also a common key early event in the development of sporadic colorectal cancers,[35] which is modelled with APC knockout mouse in which Wnt-signaling is perturbed [36]. When we analyzed the sets of effective PRC2 targets in crypts and mature enterocytes (figure 2B) separately in gene set enrichment analysis (MSigDB) [37] we found that both shared significant amount of genes with gene sets of 'upregulated genes following APC loss in mouse' ($P<2.64e-12$) and 'downregulated genes following APC loss in mouse' ($p<6.14e-5$), respectively (figure 5A). This finding suggests that consequent to APC loss and concomitant Wnt-signaling disturbance, colon epithelium is adopting more crypt/ISC –like gene expression pattern in a PRC2-dependent manner. This prompted us to analyze whether effective PRC2 targets in crypt-villus axis are also differentially expressed in colon malignancies in human. We found that significant set of effective intestinal PRC2 targets along the crypt-villus axis (hypergeometric distribution $p<0.01$) are differentially expressed in colorectal adenomas and carcinomas. Figures 5B-E show the PRC2 target expression data with genes that have altered expression both in colorectal adenomas and cancers. Thus by comparing our PRC2 target data with the gene expression data suggest that PRC2 is enacting the aberrancies in Wnt-signaling, the hallmark in in colorectal cancers [38]. Moreover, our data suggest that PRC2 participate in a malignant process where, in terms of H3K27me3 signature, epithelium in colorectal adenomas and cancers is rendered towards less mature crypt-type epithelium at the expense of mature enterocytes.

PRC2 is out-of-bounds expressed and its target genes are affected in intestine in gluten-induced crypt hyperplasia in celiac patients

We screened the expression of PRC2 protein SUZ12 in TA-region in celiac patients on gluten-free diet and the same patients after twelve weeks on gluten-containing diet. Immunohistochemical stainings with antibody against PRC2 core member SUZ12 protein showed that PRC2 is off-limits expressed in celiac gut on gluten-containing diet (figure 6A-B). As a consequence, PRC2 target genes Scinderin and SPHK1 were found downregulated in villus rudiments when celiac disease patients were consuming gluten (figure 6C-D). These results suggest that increased proliferation [39] in hyperplastic crypt in celiac patients, ignited by dietary gluten, is accompanied with the significantly less restraint PRC2 expressions and concomitant downregulation of its target genes in villus rudiments. We also monitored the bulk H3K27me3 signal in crypt-villus axis with immunohistochemistry and found uniform signal both in gluten-containing and gluten-free diets (data not shown).

To conclude, we propose a model where H3K27me3 methyltransferase activity of PRC2 in lower and middle crypt region, maintains the Wnt-signaling regulated homeostasis between crypt/ISC and villus/enterocyte compartments in healthy intestine (figure 7A**)**. In crypt hyperplasia, e.g. dietary gluten-induced in celiac patients, PRC2 is expressed off-limits and this leads to persistent silencing of its target genes in villus rudiments (figure 7B).

DISCUSSION

Our results indicate that the function of PRC2 at TA-region in the intestinal crypt-villus axis is to selectively set an epigenomic identity by labelling genes with repressive H3K27me3 mark and

therefore enforce and maintain the dichotomy for crypt and villus identities governed by Wnt-signaling (figure 7A). We have identified 90 genes regulated by PRC2 along the crypt-villus axis and among these are genes with already established roles in intestinal homeostasis and ISC maintenance e.g. LGR5, ASCL2 and Axin2. Bearing in mind that PRC2 specifically regulates genes having a function in development and signaling it is plausible to assume that also most of the identified PRC2 targets along the crypt-villus axis are causative agents in differentiation rather than just a mere consequence of it. Therefore, our work provides a resource for further studies dealing with the purportedly imperative factors maintaining the intestinal homeostasis. Many of these genes have been shown to be important in differentiation in other tissues and we summarize some of the targets here as an example.

Genes expressed in villi and repressed in crypt/ISCs by PRC2: i) *HES2.* Hes-proteins (Comprises 1-7 in humans) are basic helix-loop-helix DNA binding repressor proteins which play an essential role in the development of many organs by maintaining progenitor cells and regulating cell fate decisions [40]. Hes-proteins are effectors of Notch signaling but surprisingly HES2 was the only member from Hes-family found to be vigorously responsive to Wnt-signaling in PRC2-dependent fashion. This is interesting since from the members of Hes-family, HES2 is the one whose function is least known. Our data suggest that it is involved in enterocyte differentiation, contrary to Hes1, 3 and 5, which are all involved in secretory cell formation in the intestine [41]. ii) *MAF* is a DNA binding leucine zipper transcription factor involved in chondrocyte [42] and pancreatic beta cell differentiation [43]. Our data suggest that as a PRC2 target on crypt-villus axis it will also probably have a role in intestinal epithelial cell differentiation. iii) *Scinderin* was found downregulated in celiac patients' on gluten-containing diet. Scinderin is a Ca^{2+} -dependent actin filament severing, end capping and nucleating protein involved in differentiation of megakaryoblasts,[44] osteoclasts [45] and chondrocytes [46] but the role in Wnt-mediated enterocyte differentiation is unknown.

Genes expressed in Crypt/ISCs and repressed in villi by PRC2: i) *MNX1* is a homeobox transcription factor and mutations in this gene are linked to sacral agenesis and currarino syndrome, the latter having malformation mainly in anorectal region but sometimes duodenal atresias are present [47]. Mnx1 is involved in pancreatic development but early work with Mnx1-/- mice discovered abnormal growth in duodenum as well [48]. Our work suggests that in the small bowel MNX1 is a PRC2 target and solely expressed in duodenal crypts and probably have a role in maintaining the crypt-villus homeostasis. ii) The transcriptional repressor *ZFP503* (Znf503 in human) plays a role in mammary gland homeostasis by promoting mammary epithelial cell proliferation [49]. Intestinal crypt restricted expression of ZFP503 by PRC2 suggests similar role in the intestinal homeostasis. iii) *ETV4* is overexpressed in colorectal carcinomas and it has been shown to exert its pro-invasive and -metastatic functions through epithelial to mesenchymal transition and matrix metalloproteinase associated processes [50]. Our data showing that developmental regulator PRC2 silences ETV4 in villi accentuates the crucial role of PRC2 regulating genes involved in development and in this case the maintenance of gut homeostasis.

PRC2 target genes along the crypt-villus axis were shown to have more CpG islands in their promoters which is a very typical tendency for PRC2 targets [51]. When effective PRC2 targets were queried against differentially expressed non-PRC2 targets genes along the crypt-villus axis, we found de novo motif with the highest match to Tcf3 transcription factor to be enriched. Indeed, stimulation of the canonical Wnt-signaling pathway causes β-catenin to translocate to the nucleus and interact with Tcf/lef proteins to activate target genes [33]. It has been shown in mouse ES cells that nearly half of the genes bound by Tcf3 are also co-occupied by PRCs [52]. Our work suggest that in the intestine PRC2 is specifically involved in regulation of Tcf3 target genes in Wnt-signaling pathway.

It has been previously hypothesized that PRC-mediated gene repression might play a role in the pathogenesis of colorectal cancer [53]. This hypothesis has been set forth by the findings that PRC2 proteins interact with DNA methyltransferases [54] and that many genes that are frequently DNA hypermethylated in colorectal cancers are polycomb group target genes in human embryonic stem cells and fibroblasts [55] and in Caco-2 cancer cells [56]. Our genome-wide effective intestinal PRC2 target list assessed by H3K27me3-ChIP-Seq and Gro-Seq with non-differentiated and differentiated organoids derived from mouse duodenum now suggest that epithelium in adenomas and colorectal carcinomas adopt more crypt-like developmental status with respect to PRC2 imposed H3K27me3 signature. We also show that in celiac disease patients on gluten-containing diet causing crypt-hyperplasia is accompanied with the out-of-bounds PRC2 activity and consequent downregulation of its target genes in villi. In fact, the expression of PRC2 targets expressed in crypts (e.g. LGR5) might be also perturbed in celiac disease, as it has been shown before that number of immature proliferating TA progenitor cells expressing low levels of LGR5 were significantly increased in acute celiac disease [57].

CONCLUSION

Taken together, we have identified a PRC2 specified transcriptome, which forms an essential element in healthy gut homeostasis and aberrant PRC2 activity seems to be a common denominator in alimentary tracts diseases associated with epithelial cell hyperplasia e.g. in celiac disease (Figure 7B) or neoplasia in malignancies. Canonical intestinal stem cell effectors (e.g. Lgr5 and Ascl2) were found to be targets for developmental regulator PRC2, and thus identified novel PRC2 targets are also purportedly bona fide regulators of intestinal stem cell self-renewal and differentiation. Inhibition of methyltransferase activity of EZH2 component in PRC2 has emerged as a potential target for

development of novel therapeutic strategies in cancers. However, our data raises concerns for its feasibility in colorectal cancers as adverse pro-oncogenic effects might arise due to the pro-stemness and pro-differentiation functions of PRC2 in intestine.

ACKNOWLEDGEMENTS

Funding: This work was supported by Academy of Finland (265575), Päivikki and Sakari Sohlberg Foundation, Sigrid Jusélius Foundation, Tekes – The Finnish Funding Agency for Innovation (658/31/2015) and Competitive State Research Financing of the Expert Responsibility Area of the Tampere University Hospital, Grant 9T040. M.U.K was supported by the Academy of Finland, Sigrid Jusélius Foundation, Finnish Foundation for Cardiovascular Research and Finnish Cultural Foundation. We thank The Sequencing Service GeneCore Sequencing Facility (EMBL, http://www.genecore.embl.de) for DNA sequencing. **Author contributions:** K.V. conceived the project, performed mini-gut cultures and ChIP-Seq and RT-qPCR experiments and conducted data analysis. M.O. performed bioinformatic analyses on ChIP- and GRO-Seq data, immunohistochemical stainings, mechanical villus-crypt separations, RT-qPCR experiments and statistical tests. M.U.K. performed GRO-Seq experiments and analyses. A.P., K.K. and M.M. acquired biopsies. K.V. drafted and prepared the manuscript with contributions from M.O., A.P., K.K., K.L., M.M. and M.U.K. K.V. and M.M. acquired funding for the project. All authors accepted the final version of the manuscript. **Conflict of interest:** None. **Accession number:** Data series entry GSE78761 for the ChIP- and Gro-Seq data is accepted in GEO.

REFERENCES

1. Schuettengruber B, Cavalli G. Recruitment of polycomb group complexes and their role in the dynamic regulation of cell fate choice. Development 2009;136:3531–3542.
2. Cao R, Wang L, Wang H, et al. Role of histone H3 lysine 27 methylation in Polycomb-group silencing. Science 2002;298:1039–1043.
3. Lee TI, Jenner RG, Boyer LA, et al. Control of Developmental Regulators by Polycomb in Human Embryonic Stem Cells. Cell 2006;125:301–313.
4. Bernstein E, Duncan EM, Masui O, et al. Mouse polycomb proteins bind differentially to methylated histone H3 and RNA and are enriched in facultative heterochromatin. Mol. Cell. Biol. 2006;26:2560–2569.
5. Bracken AP, Helin K. Polycomb group proteins: navigators of lineage pathways led astray in cancer. Nat. Rev. Cancer 2009;9:773–784.
6. Barker N. Adult intestinal stem cells: critical drivers of epithelial homeostasis and regeneration. Nat Rev Mol Cell Biol 2014;15:19–33.
7. Diosdado B, Oort E van, Wijmenga C. "Coelionomics": towards understanding the molecular pathology of coeliac disease. Clin. Chem. Lab. Med. 2005;43:685–95.
8. Lee TI, Jenner RG, Boyer LA, et al. Control of developmental regulators by Polycomb in human embryonic stem cells. Cell 2006;125:301–13.
9. Wang L, Jin Q, Lee J-E, et al. Histone H3K27 methyltransferase Ezh2 represses Wnt genes to facilitate adipogenesis. Proc. Natl. Acad. Sci. U. S. A. 2010;107:7317–7322.
10. Pinto D, Gregorieff A, Begthel H, et al. Canonical Wnt signals are essential for homeostasis of the intestinal epithelium. Genes Dev. 2003;17 :1709–1713.
11. Kim T-H, Li F, Ferreiro-Neira I, et al. Broadly permissive intestinal chromatin underlies lateral inhibition and cell plasticity. Nature 2014;506:511–5.
12. Chiacchiera F, Rossi A, Jammula S, et al. Polycomb Complex PRC1 Preserves Intestinal Stem Cell Identity by Sustaining Wnt/beta-Catenin Transcriptional Activity. Cell Stem Cell 2016;18:91–103.

13. Sato T, Stange DE, Ferrante M, et al. Long-term expansion of epithelial organoids from human colon, adenoma, adenocarcinoma, and Barrett's epithelium. Gastroenterology 2011;141:1762–72.

14. Leushacke M, Barker N. Ex vivo culture of the intestinal epithelium: strategies and applications. Gut 2014;63 :1345–1354.

15. Halttunen T, Marttinen a, Rantala I, et al. Fibroblasts and transforming growth factor beta induce organization and differentiation of T84 human epithelial cells. Gastroenterology 1996;111:1252–62.

16. Lähdeaho M-L, Mäki M, Laurila K, et al. Small- bowel mucosal changes and antibody responses after low- and moderate-dose gluten challenge in celiac disease. BMC Gastroenterol. 2011;11:129.

17. Core LJ, Waterfall JJ, Lis JT. Nascent RNA sequencing reveals widespread pausing and divergent initiation at human promoters. Science (80-.). 2008;322:1845–1848.

18. Kaikkonen MU, Niskanen H, Romanoski CE, et al. Control of VEGF--a transcriptional programs by pausing and genomic compartmentalization. Nucleic Acids Res 2014;42:12570–12584.

19. Mantyla E, Salokas K, Oittinen M, et al. Promoter targeted histone acetylation of chromatinized parvoviral genome is essential for infection progress. J. Virol. 2016.

20. Qi W, Chan H, Teng L, et al. Selective inhibition of Ezh2 by a small molecule inhibitor blocks tumor cells proliferation. Proc. Natl. Acad. Sci. 2012;109 :21360–21365.

21. Benoit YD, Lepage MB, Khalfaoui T, et al. Polycomb repressive complex 2 impedes intestinal cell terminal differentiation. J. Cell Sci. 2012;125:3454–3463.

22. Sato T, Vries RG, Snippert HJ, et al. Single Lgr5 stem cells build crypt-villus structures in vitro without a mesenchymal niche. Nature 2009;459:262–5.

23. Uhlen M, Fagerberg L, Hallstrom BM, et al. Tissue-based map of the human proteome. Science (80-.). 2015;347:1260419–1260419.

24. Barker N, Es JH van, Kuipers J, et al. Identification of stem cells in small intestine and colon by marker gene Lgr5. Nature 2007;449:1003–1007.

25. Flier LG van der, Gijn ME van, Hatzis P, et al. Transcription Factor Achaete Scute-Like 2 Controls Intestinal Stem Cell Fate. Cell 2009;136:903–912.

26. Furstenberg RJ von, Gulati AS, Baxi A, et al. Sorting mouse jejunal epithelial cells with CD24 yields a population with characteristics of intestinal stem cells. Am. J. Physiol. Gastrointest. Liver Physiol. 2011;300:G409–17.

27. Merlos-Suárez A, Barriga FM, Jung P, et al. The intestinal stem cell signature identifies colorectal cancer stem cells and predicts disease relapse. Cell Stem Cell 2011;8:511–524.

28. Fafilek B, Krausova M, Vojtechova M, et al. Troy, a tumor necrosis factor receptor family member, interacts with Lgr5 to inhibit Wnt signaling in intestinal stem cells. Gastroenterology 2013;144:381–391.

29. Jho E, Zhang T, Domon C, et al. Wnt/beta-catenin/Tcf signaling induces the transcription of Axin2, a negative regulator of the signaling pathway. Mol. Cell. Biol. 2002;22:1172–83.

30. Terahara K, Yoshida M, Igarashi O, et al. Comprehensive gene expression profiling of Peyer's patch M cells, villous M-like cells, and intestinal epithelial cells. J. Immunol. 2008;180:7840–7846.

31. Boyer L a, Plath K, Zeitlinger J, et al. Polycomb complexes repress developmental regulators in murine embryonic stem cells. Nature 2006;441:349–353.

32. Orlando D a., Guenther MG, Frampton GM, et al. CpG island structure and trithorax/polycomb chromatin domains in human cells. Genomics 2012;100:320–326.

33. Cadigan KM. Wnt signaling - 20 Years and counting. In: *Trends in Genetics*.Vol 18.; 2002:340–342.

34. Kinzler KW, Nilbert MC, Su LK, et al. Identification of FAP locus genes from chromosome 5q21. Science 1991;253:661–665.

35. Kinzler KW, Vogelstein B. Lessons from Hereditary Colorectal Cancer. Cell 1996;87:159–170.

36. Sansom OJ, Reed KR, Hayes AJ, et al. Loss of Apc in vivo immediately perturbs Wnt signaling, differentiation, and migration. Genes Dev. 2004;18:1385–1390.

37. Subramanian A, Tamayo P, Mootha VK, et al. Gene set enrichment analysis: a knowledge-based approach for interpreting genome-wide expression profiles. Proc. Natl. Acad. Sci. U. S. A. 2005;102:15545–50.

38. Segditsas S, Tomlinson I. Colorectal cancer and genetic alterations in the Wnt pathway. Oncogene 2006;25:7531–7.

39. Maiuri L, Ciacci C, Raia V, et al. FAS engagement drives apoptosis of enterocytes of coeliac patients. Gut 2001;48:418–424.

40. Kageyama R, Ohtsuka T, Kobayashi T. The Hes gene family: repressors and oscillators that orchestrate embryogenesis. Development 2007;134:1243–1251.

41. Ueo T, Imayoshi I, Kobayashi T, et al. The role of Hes genes in intestinal development, homeostasis and tumor formation. Development 2012;139:1071–1082.

42. Hong E, Cesare PE Di, Haudenschild DR. Role of c-Maf in Chondrocyte Differentiation: A

Review. Cartilage 2011;2:27–35.

43. Aramata S, Han S-I, Kataoka K. Roles and regulation of transcription factor MafA in islet beta-cells. Endocr. J. 2007;54:659–666.

44. Zunino R, Li Q, Rosé SD, et al. Expression of scinderin in megakaryoblastic leukemia cells induces differentiation, maturation, and apoptosis with release of plateletlike particles and inhibits proliferation and tumorigenesis. Blood 2001;98:2210–2219.

45. Jiang H, Wang Y, Viniegra A, et al. Adseverin plays a role in osteoclast differentiation and periodontal disease-mediated bone loss. FASEB J. 2015;29 :2281–2291.

46. Nurminsky D, Magee C, Faverman L, et al. Regulation of chondrocyte differentiation by actin-severing protein adseverin. Dev. Biol. 2007;302:427–437.

47. Ross AJ, Ruiz-Perez V, Wang Y, et al. A homeobox gene, HLXB9, is the major locus for dominantly inherited sacral agenesis. Nat. Genet. 1998;20:358–361.

48. Li H, Arber S, Jessell TM, et al. Selective agenesis of the dorsal pancreas in mice lacking homeobox gene Hlxb9. Nat. Genet. 1999;23:67–70.

49. Shahi P, Slorach EM, Wang C-Y, et al. The Transcriptional Repressor ZNF503/Zeppo2 Promotes Mammary Epithelial Cell Proliferation and Enhances Cell Invasion. J. Biol. Chem. 2015;290 :3803–3813.

50. Mesci A, Taeb S, Huang X, et al. Pea3 expression promotes the invasive and metastatic potential of colorectal carcinoma. World J. Gastroenterol. 2014;20:17376–87.

51. Orlando DA, Guenther MG, Frampton GM, et al. CpG island structure and trithorax/polycomb chromatin domains in human cells. Genomics 2012;100:320–6.

52. Cole MF, Johnstone SE, Newman JJ, et al. Tcf3 is an integral component of the core regulatory circuitry of embryonic stem cells. Genes Dev. 2008;22 :746–755.

53. Goel A, Boland CR. Epigenetics of colorectal cancer. Gastroenterology 2012;143:1442–1460.e1.

54. Viré E, Brenner C, Deplus R, et al. The Polycomb group protein EZH2 directly controls DNA methylation. Nature 2006;439:871–4.

55. Ohm JE, McGarvey KM, Yu X, et al. A stem cell-like chromatin pattern may predispose tumor suppressor genes to DNA hypermethylation and heritable silencing. Nat Genet 2007;39:237–242.

56. Schlesinger Y, Straussman R, Keshet I, et al. Polycomb-mediated methylation on Lys27 of histone H3 pre-marks genes for de novo methylation in cancer. Nat Genet 2007;39:232–236.

57. Senger S, Sapone A, Fiorentino MR, et al. Celiac Disease Histopathology Recapitulates Hedgehog Downregulation, Consistent with Wound Healing Processes Activation. PLoS One

2015;10:e0144634.

58. Sabates-Bellver J, Flier LG Van der, Palo M de, et al. Transcriptome profile of human colorectal adenomas. Mol. Cancer Res. 2007;5:1263–1275.

59. Khamas A, Ishikawa T, Shimokawa K, et al. Screening for epigenetically masked genes in colorectal cancer using 5-aza-2′-deoxycytidine, microarray and gene expression profile. Cancer Genomics and Proteomics 2012;9:67–75.

FIGURE LEGENDS

Figure 1. PRC2 is expressed in crypt/ISCs-TA region and regulates enterocyte differentiation *in vitro*. (A) Quantitative reverse transcription PCR (qRT-PCR) showing the expression (mean and SD, n=3) of intestinal cell type markers in T84 cells grown in matrigel and treated with 5μM of EZH2 inhibitor or DMSO (vehicle). Bars represent the expression change after 6 days of EZH2 inhibition relative to DMSO treated cells. (LGR5, ISCs; ALPI, enterocytes; LYZ, paneth cells; CHGA, secretory cells; MUC2, goblet cells). *Right*, Western blotting of H3K27me3 and H3 (loading control) showing the decrease of bulk H3K27me3 level in cells treated with EZH2 inhibitor. (B) qRT-PCR (mean and SD, n=3), as in *A,* for mouse mini-gut organoid cultures grown in stem cell media (WENRCV) and treated with 5μM of EZH2 inhibitor or DMSO. Significant p-values in t-tests are shown in A and B. (C) qRT-PCR measurements of PRC2 members and GATA4 (control) in mouse mini-gut cultures grown in stem cell media (WENRC) and enterocyte differentiation media (ENRI). (D) qRT-PCR (mean and SD, n=3) from mechanically separated crypt (LGR5-marker) and villus (ALPI-marker) epithelium from mouse. Bars represent expression of PRC2 members SUZ12 and EZH2 in crypt/ISCs-TA region relative to villi.

Figure 2. PRC2 defines crypt and villus domains by marking genes with repressive H3K27me3. (A) Gene expression heat maps showing genes upregulated in mature enterocytes (magenta) and in intestinal stem cells (ISC)/crypt cells (green) studied by global run-on-sequencing (GRO-Seq) from mouse intestinal mini-gut organoids grown in enterocyte differentiation (ENRI) and stem cell media (WENRC) (two mice analyzed in batch as biological replicates; see methods). (B) Heat maps depicting subset of genes regulated by PRC2 (screened by H3K27me3 ChIP-Seq) on crypt-villus axis. (C) Composite enrichment profile of H3K27me3 at found PRC2 target genes that are silenced in crypts/ISCs (green) and later activated in enterocytes (magenta). (D) Composite enrichment profile of H3K27me3 at genes which are expressed in crypts/ISCs (green) and later silenced by PRC2 in enterocytes (magenta). Plots in C and D show average fold-enrichment (normalized signal from H3K27me3-ChIP-Seq versus whole genomic DNA). (E) Scatter blot demonstrating the genome-wide change in H3K27me3 occupancy during the differentiation of crypt/ISCs to mature enterocytes. Blue dots represents all normalized differential H3K27me3 ChIP-Seq peaks near protein coding genes of the mouse genome. Only the highest scoring peak per gene is shown. Red colored triangles denote the genes having significant gene expression difference measured by GRO-Seq and arrows quantitatively illustrate the gene expression difference in enterocytes relative to crypts/ISCs (up=activation, down=repression). Only the highest scoring peak per gene is shown. X-axis: H3K27me3 ChIP-Seq normalized tag count (log_2) in organoids grown in WENRC i.e. crypt/ISCs and Y-axis: H3K27me3 ChIP-Seq normalized tag count (log_2) in organoids grown in ENRI i.e. mature enterocytes.

Figure 3. PRC2 regulates the intestinal stem cell niche. (A) *Above*, H3K27me3 occupancy at canonical intestinal stem cell marker genes and wnt-signaling regulators in enterocytes (magenta) and in crypt/ISCs (green) (Y-axis: normalized tag count). *Below*, pre-mRNA expressions from corresponding genes are shown in enterocytes and in crypt/ISCs (Y-axis: normalized tag count). (B) Data (as in A) for

some of the novel PRC2 targets specifically repressed in crypt/ISCs. Immunohistochemical staining for the corresponding genes (obtained from *Protein Atlas* –database, www.proteinatlas.org) suggest that the expression gradient maintained by PRC2 is also occurring in humans *in vivo*. (C) Data (as in A and B) for the selected PRC2 targets in mature enterocytes. Both ChIP- and GRO-Seq data are shown as USCS genome browser snapshots aligned in corresponding genes (in A, B and C). (D) qRT-PCR data from crude mechanically isolated mouse crypt and villus fractions (mean and SD, n=3) for the PRC2 targets silenced in enterocytes.

Figure 4. PRC2 target genes are involved in intestinal homeostasis and enterocyte differentiation. (A) -log P-values for the enrichment of GO & pathway-categories in the set of genes that are silenced by PRC2 in crypts/ISCs. (B) –log P-values for the enrichment of GO-categories in the set of genes that are silenced by PRC2 in mature enterocytes. (C) Best (p- and match-value combined) enriched *de novo* transcription target motif within PRC2-dependent crypt and villus specific genes when PRC2-independent crypt and villus specific genes were used as a background. (D) The portion of genes with zero, one or two and more CpG islands in mouse genome in general (white bar) and crypt and villus specific genes not regulated by PRC2 (gray bar) and crypt and villus specific genes regulated by PRC2 (black bar).

Figure 5. Gene expression analyses suggest that aberrant stemness fostering PRC2 activity is implicated in adenomas and colorectal cancers. (A) Molecular Signatures Database (MSigDB) analyses with effective PRC2 targets in crypts/ISCs and mature enterocytes. P-values show the significance of the amount of shared genes between indicated queried and repository data sets. (B&C) Box plot charts of intestinal PRC2 targets and their significantly altered gene expression levels in adenomas. Microarray data is obtained from Gene Expression Omnibus (GEO) GDS2947[58] data set. Black lines indicate the median expression in 32 patients and upper and lower edges of the boxes mark the

boundaries of 3rd and 1st quartiles. Tukey whiskers depict the lowest and highest data points within 1.5 interquartile range. Gene expressions from colorectal adenomas (pink) and normal mucosas (green) from 32 patients are shown on log scale. (D&E) The expression of the same genes as above, obtained from GDS4382[59], in colorectal tumor (magenta) and adjacent non-cancerous tissues (green) from 17 patients.

Figure 6. PRC2 is out-of-bounds expressed and its enterocytic target genes are repressed in celiac patients on gluten-containing diet. (A) Representative immunohistochemical staining with PRC2 core member SUZ12 on duodenal biopsy sections obtained from celiac patient on gluten-free-diet (GFD) and from the same patient after 12 weeks on gluten containing-diet. (B) Line chart illustrates the quantitated SUZ12 immunohistochemical staining data from six patients on GFD and after gluten containing-diet. Dots represent mean and above is shown the p-value for t-test. (C) Representative immunohistochemical stainings for PRC2 targets Scinderin and (D) Sphk1 in celiac patients on GFD and on gluten-containing diet showing decrease in their expression upon gluten induced crypt hyperplasia

Figure 7. Proposed model for the PRC2 function in maintaining the intestinal homeostasis and aberrancies therein in crypt hyperplasia. (A) At TA-region in the healthy intestine PRC2 (composed of core members SUZ12, EZH2 and EED proteins) impose crypt- and villus specific H3K27me3 signatures and set the dichotomy for these two compartments. Solid line arrows illustrate how PRC2 reigned transcriptional regulation takes place in lower and middle crypt region and dashed arrow indicate that repressive H3K27me3 is passively maintained in crypt genes once enterocytes have reached the terminal differentiation compartment in the upper crypt and migrate further to the villus. (B) In diseases inflicting crypt hyperplasia (e.g. celiac disease) PRC2 is expressed off-limits and

consequently its target genes in villi are less expressed possibly because they still retain some H3K27me3 modification.

Supplemental figure 1. Optimizing mouse mini-gut culturing conditions to mimic intestinal crypt-villus-axis. (A) qRT-PCR showing the expression (mean ± SD) of intestinal cell type markers relative to GAPDH in mouse mini-gut organoids grown in matrigel and basal culturing media (BCM, see methods) supplemented with W = Wnt3a, E = Egf, N = Noggin, R = R-Spondin, C = CHIR99021, V = Valproic acid, I = IWP2, D = DAPT. (B) Relative expression of intestinal cell type markers (mean ± SD), measured by qRT-PCR, for chosen culturing conditions WENRC and ENRI for Crypt+ISC and enterocyte, respectively. Bars indicate the expression of genes in ENRI/enterocyte conditions relative to WENRC/Crypt+ISC conditions. (C) Representative microscopic pictures of organoids grown in WENRC and ENRI culturing conditions.

Supplemental figure 2. Heat maps of histone modification H3K27me3 signal (A) and histone 3 as a control (B) within +-10 kb of all transcriptional start sites (TSSs) in mouse genome in mini-guts grown in WENRC and ENRI media. Above the heat maps composite enrichment profiles of H3K27me3 occupancy across the TSSs are shown (Y-axis, fold enrichment of H3K27me3).

Supplemental figure 3. Example of genes differentially expressed in mini-guts and displaying also crypt and villus specific expression pattern in human *in vivo* when queried from Protein Atlas database (www.proteinatlas.org). (A) Showing data for the genes expressed in villus and (B) for the genes expressed in crypts. Above each IHC stainings (obtained from Protein Atlas database) corresponding

pre-mRNA expression detected in Gro-Seq from the given locus are shown as USCS genome browser snapshots (red, grown in ENRI (villus/enterocyte) conditions; green, grown in WENRC (Crypt/ISCs) conditions).

Legend for Graphical Abstract. Schematic representation of the role of Polycomb Repressive Complex 2 (PRC2) on enacting the Wnt/β-catenin signaling and regulating the homeostasis of intestinal stem cell self-renewal and differentiation. At transit amplifying (TA) region PRC2 selectively set an epigenomic identity by labelling genes with repressive H3K27me3 mark and therefore enforce and maintain the dichotomy for crypt and villus identities. This manuscript suggest that PRC2 contributes to the stemness instigation process in epithelial hyperplasia in celiac disease and in neoplasia in colorectal carcinoma. Schematic scatter blot on the right demonstrates the genome-wide change in H3K27me3 occupancy during the differentiation of crypt/Intestinal stem cells to mature enterocytes. Blue dots represents all normalized differential H3K27me3 ChIP-Seq peaks near protein coding genes of the mouse genome (above genes silenced in crypts and below genes silenced in villi). Red colored triangles denote the genes having significant gene expression difference measured by GRO-Seq and arrows quantitatively illustrate the gene expression difference in enterocytes relative to crypts/ISCs (up=activation, down=repression).

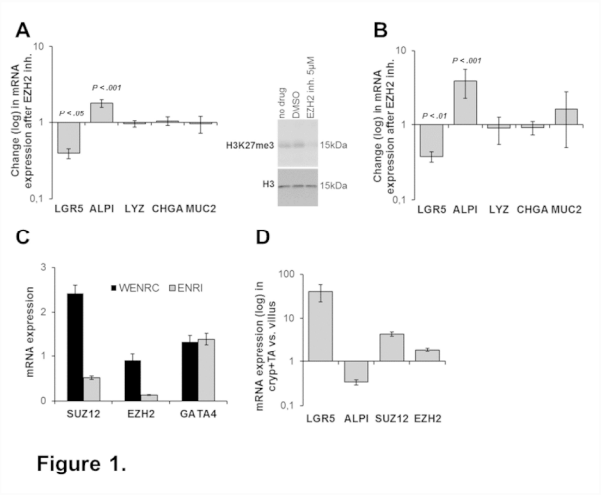

Figure 1.

Figure 1. PRC2 is expressed in crypt/ISCs-TA region and regulates enterocyte differentiation in vitro.
Figure 1
297x420mm (300 x 300 DPI)

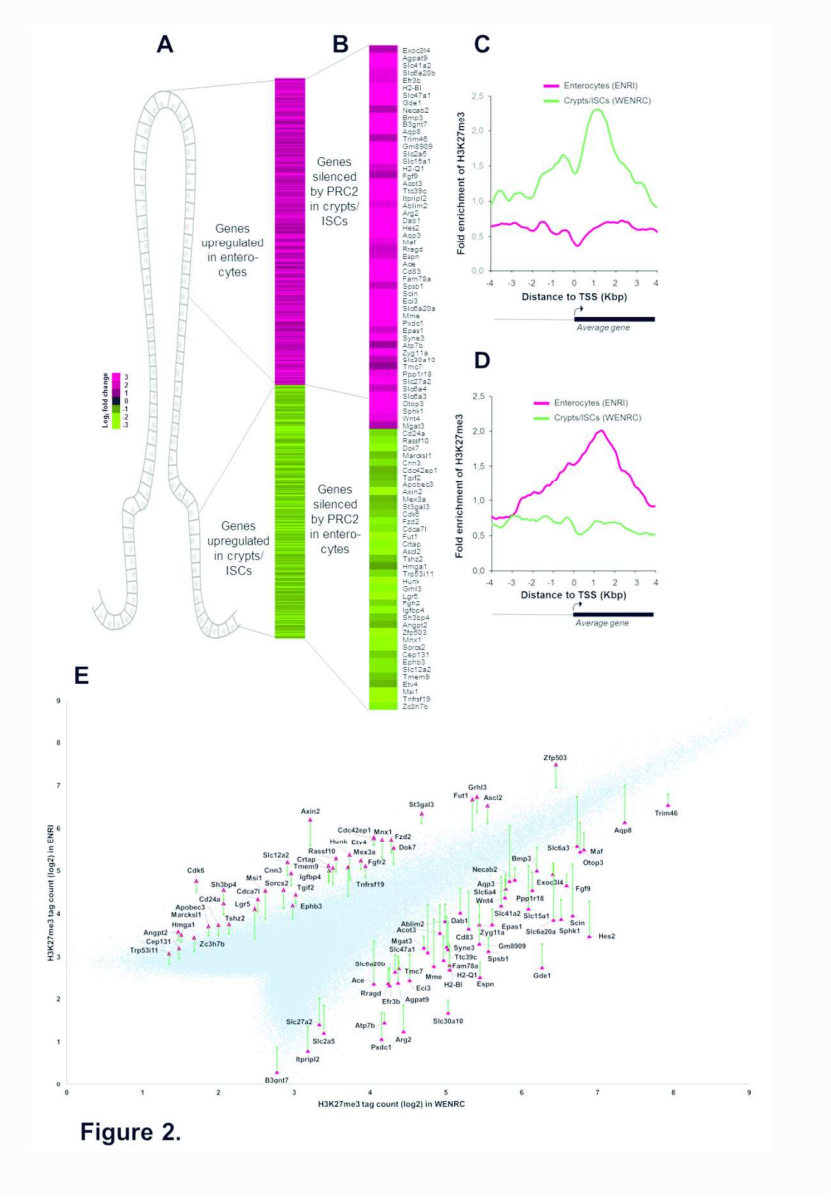

Figure 2.

Figure 2. PRC2 defines crypt and villus domains by marking genes with repressive H3K27me3.
Figure 2
250x359mm (300 x 300 DPI)

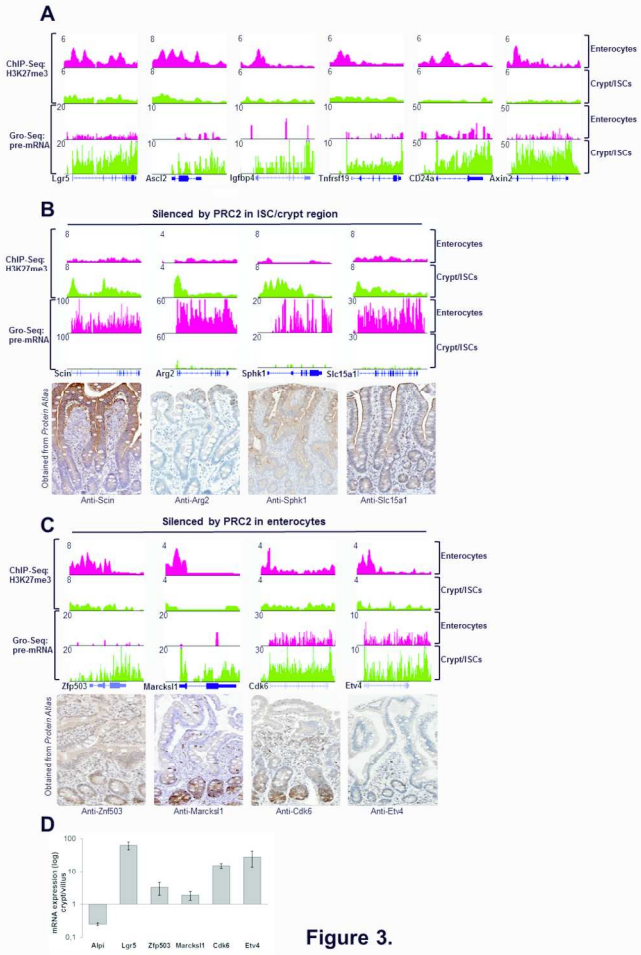

Figure 3.

Figure 3. PRC2 regulates the intestinal stem cell niche.
Figure 3
297x420mm (300 x 300 DPI)

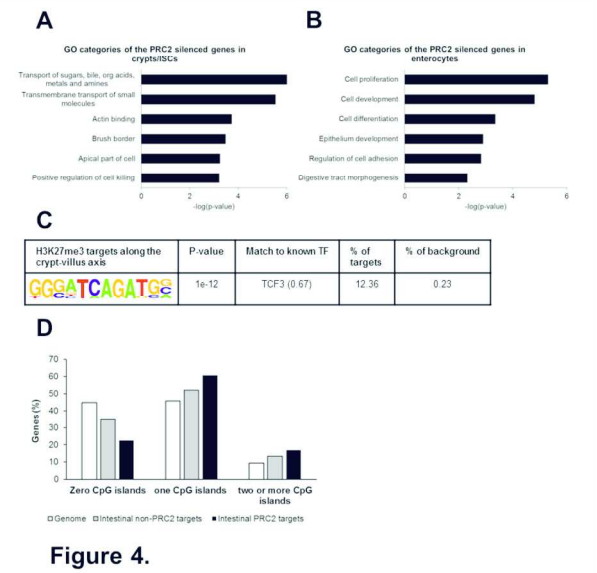

Figure 4.

Figure 4. PRC2 target genes are involved in intestinal homeostasis and enterocyte differentiation.
Figure 4
297x420mm (300 x 300 DPI)

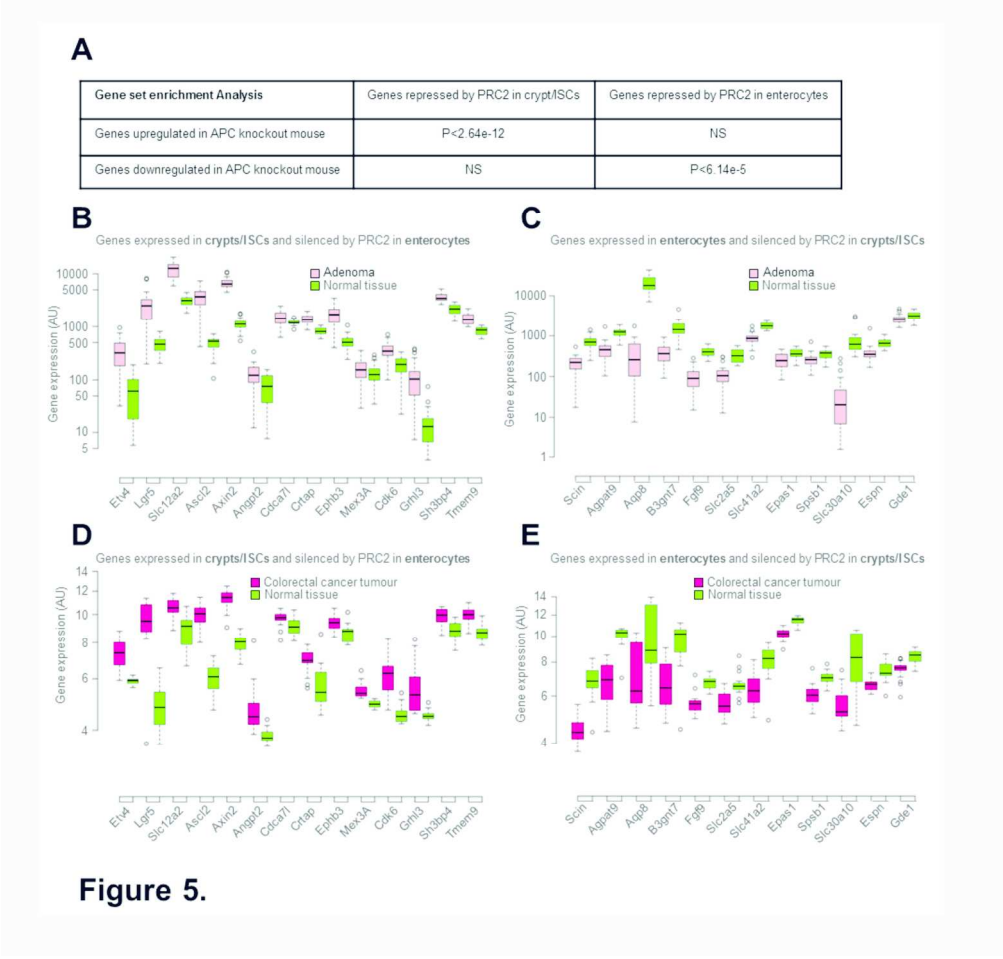

Figure 5. Gene expression analyses suggest that aberrant stemness fostering PRC2 activity is implicated in adenomas and colorectal cancers.

Figure 5

165x158mm (300 x 300 DPI)

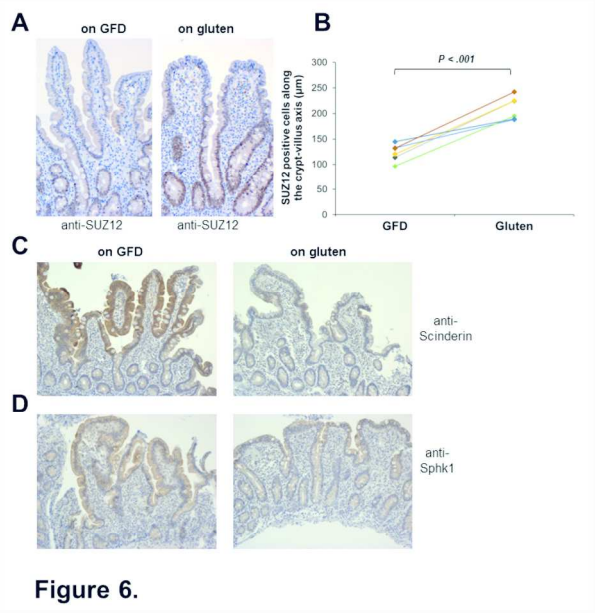

Figure 6.

Figure 6. PRC2 is out-of-bounds expressed and its enterocytic target genes are repressed in celiac patients on gluten-containing diet.

Figure 6
297x420mm (300 x 300 DPI)

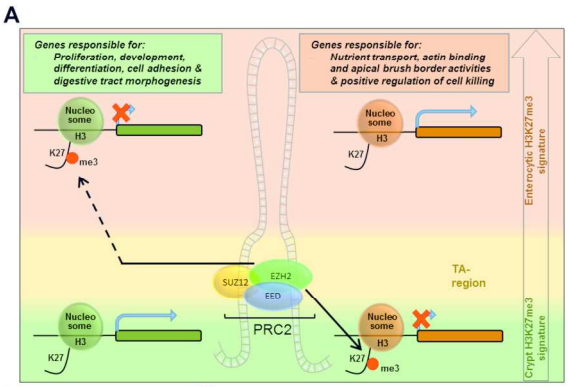

Figure 7.

Figure 7. Proposed model for the PRC2 function in maintaining the intestinal homeostasis and aberrancies therein in crypt hyperplasia.
Figure 7
297x420mm (300 x 300 DPI)

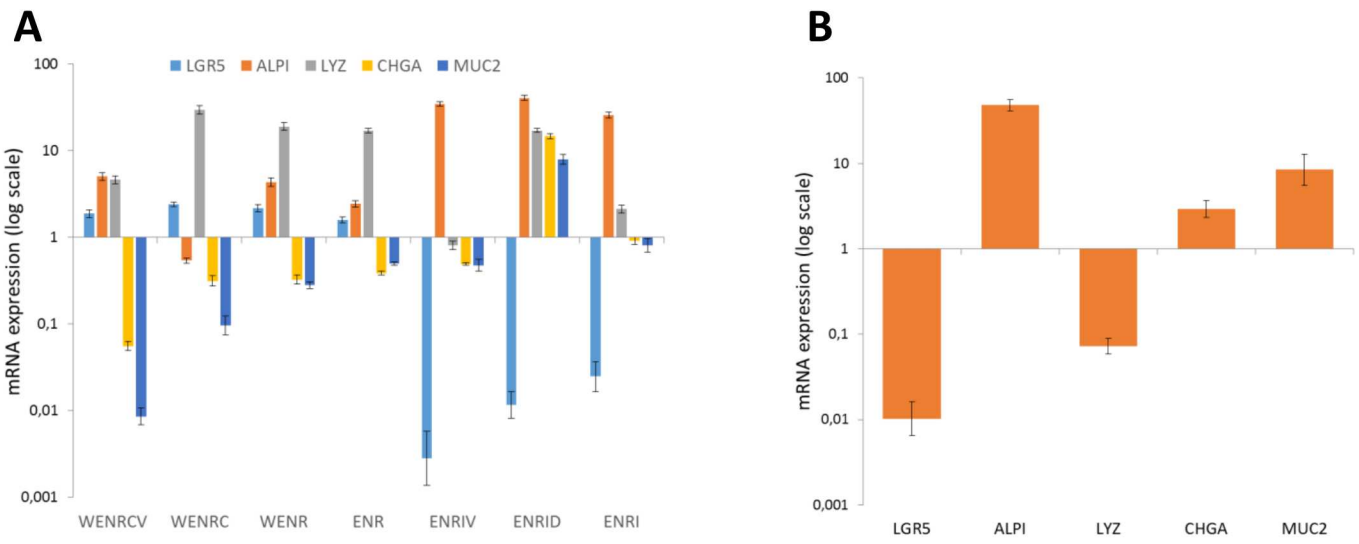
A
LGR5
ALPI
LYZ
CHGA
MUC2
mRNA expression (log scale)
100
10
1
0,1
0,01
0,001
WENRCV
WENRC
WENR
ENR
ENRIV
ENRID
ENRI
B
mRNA expression (log scale)
100
10
1
0,1
0,01
0,001
LGR5
ALPI
LYZ
CHGA
MUC2

C

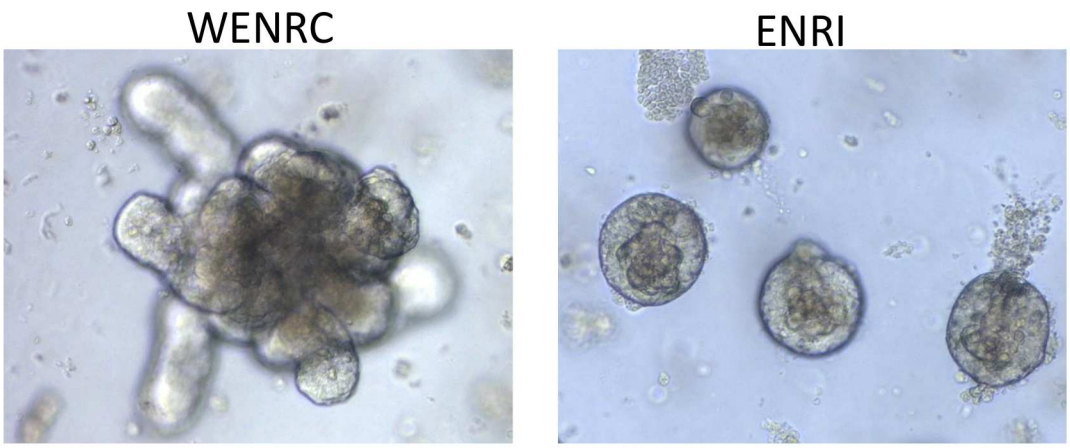
WENRC
ENRI

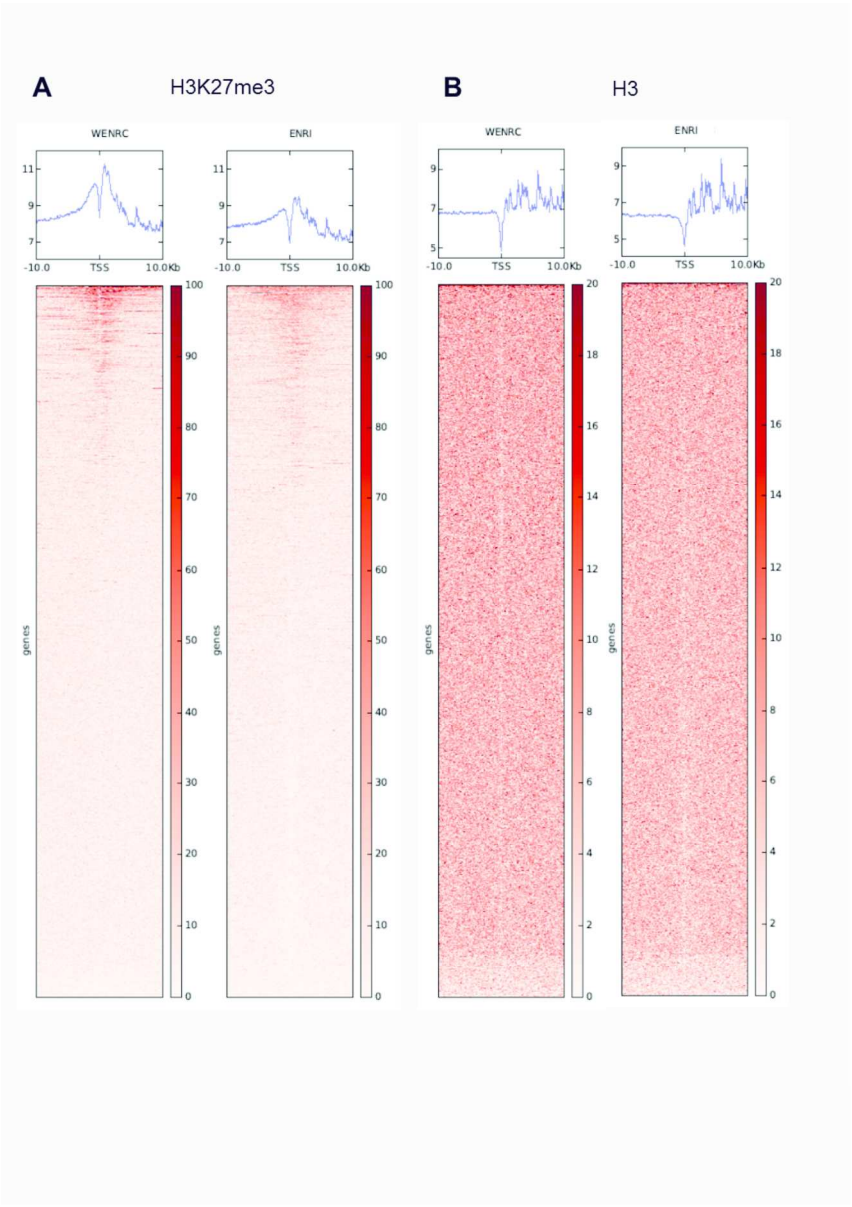

297x420mm (300 x 300 DPI)

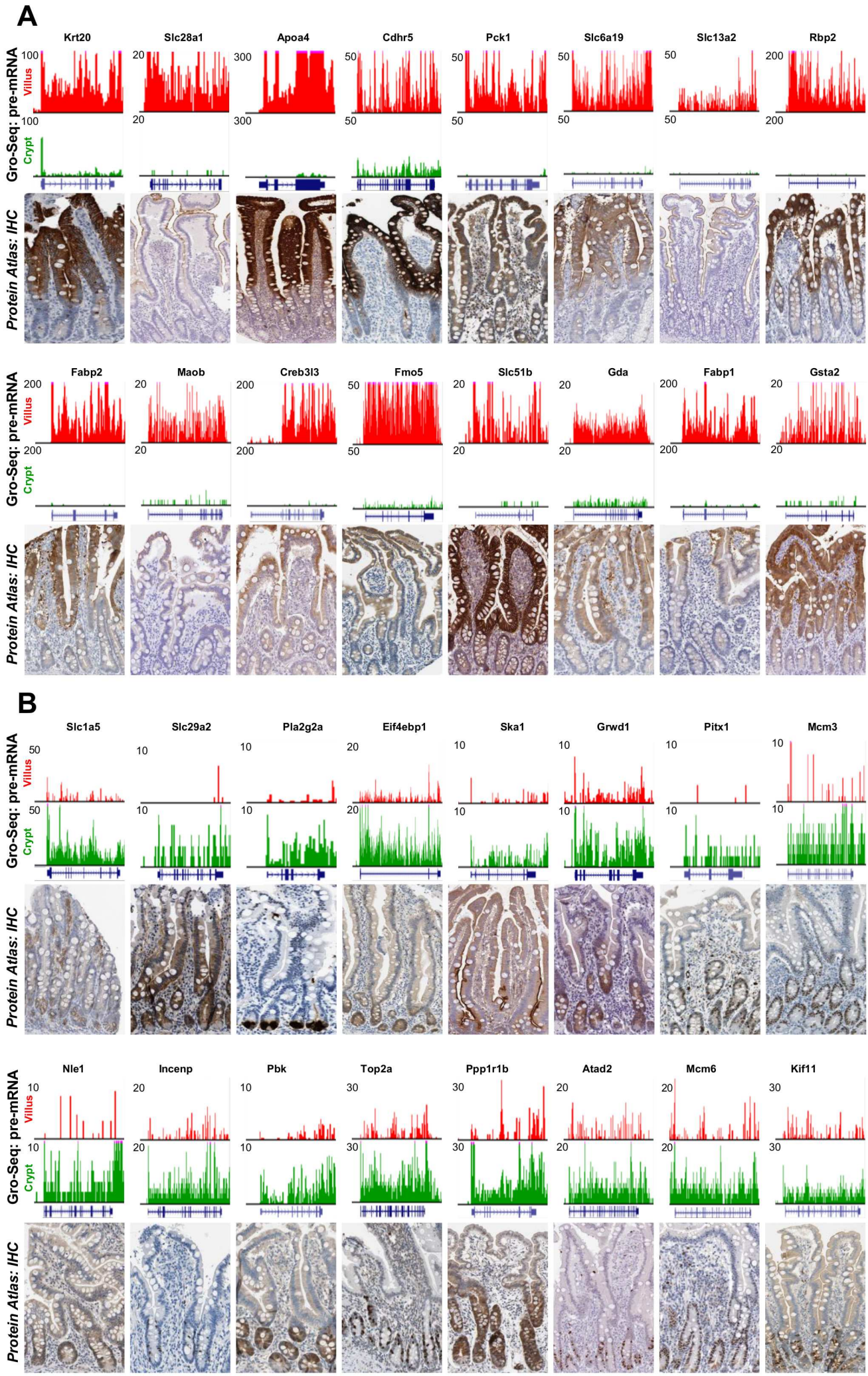
A
Krt20
Slc28a1
Apoa4
Cdhr5
Pck1
Slc6a19
Slc13a2
Rbp2
Gro-Seq: pre-mRNA
Villus
Crypt
Protein Atlas: IHC
Fabp2
Maob
Creb3l3
Fmo5
Slc51b
Gda
Fabp1
Gsta2
B
Slc1a5
Slc29a2
Pla2g2a
Eif4ebp1
Ska1
Grwd1
Pitx1
Mcm3
Nle1
Incenp
Pbk
Top2a
Ppp1r1b
Atad2
Mcm6
Kif11

Genes upregulated in mini-guts in (ENRI) enterocyte-differentiation culturing conditions

Acc ID	NAME	WENRC vs. ENRI logFC; Protein coding FC => 1, P < 0.05, RPKM > 0.5
NM_011036	Reg3b	9.8
NM_026925	Pnlip	8.237
NM_026918	Zg16	7.338
NM_001161741	Reg3d	7.269
NM_011259	Reg3a	7.194
NM_205822	Omt2b	6.717
NM_016689	Aqp3	6.68
NM_011044	Pck1	6.664
NM_139142	Slc6a20a	6.511
NM_001029935	Trim38	6.479
NM_009692	Apoa1	6.389
NM_009042	Reg1	6.209
NM_001146196	Scin	6.135
NM_010020	Slc6a3	6.052
NM_007468	Apoa4	5.713
NM_007718	Ccr1l1	5.702
NM_026183	Slc47a1	5.68
NM_172801	Otop2	5.65
NM_001289462	Mme	5.649
NM_010002	Cyp2c38	5.636
NM_008116	Ggt1	5.586
NM_001004184	Slc28a1	5.495
NM_023219	Slc5a4b	5.461
NM_019481	Slc13a1	5.424
NM_028878	Slc6a19	5.407
NM_009258	Spink3	5.373
NM_022411	Slc13a2	5.352
NM_023493	Cml5	5.281
NM_146802	Olfr902	5.239
NM_013467	Aldh1a1	5.208
NM_008191	Guca2b	5.16
NM_053079	Slc15a1	5.159
NM_009034	Rbp2	5.133
NM_009467	Ugt2b5	5.094
NM_009598	Ace	5.022
NM_001001809	Olfr218	5.006
NM_207554	Olfr257	5.006
NM_001011778	Olfr285	5.006
NM_001011542	Olfr1532-ps1	4.969
NM_007980	Fabp2	4.932
NM_001150749	Rdh7	4.876
NM_026096	Hypm	4.865
NM_145474	Cyp2d34	4.853
NM_146278	Olfr729	4.853
NM_010006	Cyp2d9	4.839
NM_001085529	Slc2a7	4.806
NM_001004141	Cyp2j11	4.778
NM_023455	Nat8	4.731
NM_147018	Olfr1056	4.717
NM_146332	Olfr135	4.717
NM_001289755	Apoc3	4.708
NM_027780	Slc6a19os	4.697
NM_001111286	Omt2a	4.693
NM_010214	Fhl4	4.673
NM_054085	Alpk3	4.609
NM_146617	Olfr307	4.561
NM_146433	Olfr994	4.561
NM_199366	Gal3st2	4.544
NM_023256	Krt20	4.525
NM_007934	Enpep	4.514
NM_011260	Reg3g	4.51
NM_144930	Ces1f	4.501
NM_001142539	Gm9992	4.499
NM_146198	Slc5a11	4.488
NM_001038660	Slc7a15	4.483

NM_001277944	Apoc2	4.482
NM_134154	Slc25a45	4.469
NM_001289915	Cd83	4.461
NM_001168590	2010106E10Rik	4.443
NM_001109045	Aqp8	4.413
NM_008574	Smcp	4.402
NM_001163503	2010001E11Rik	4.391
NM_146582	Olfr1046	4.384
NM_019476	Olfr159	4.384
NM_146858	Olfr275	4.384
NM_146950	Olfr341	4.384
NM_207620	Olfr774	4.384
NM_009969	Csf2	4.371
NM_023566	Muc2	4.337
NM_172778	Maob	4.334
NM_145365	Creb3l3	4.323
NM_053165	Clec2h	4.312
NM_001161763	Fmo5	4.309
NM_001201470	Papss2	4.295
NM_027363	Chp2	4.237
NM_178933	Slc51b	4.235
NM_001130513	Ace2	4.227
NM_008236	Hes2	4.211
NM_007818	Cyp3a11	4.185
NM_021375	Rhbg	4.179
NM_007876	Dpep1	4.146
NM_001081211	Ptafr	4.131
NM_001277847	Treh	4.073
NM_001145390	Gm766	4.066
NM_023860	Krtap5-3	4.058
NM_001111094	Btnl1	4.021
NM_001081137	Sis	4.017
NM_008631	Mt4	3.984
NM_008061	G6pc	3.971
NM_011333	Ccl2	3.936
NM_007409	Adh1	3.929
NM_011996	Adh4	3.899
NM_011128	Pnliprp2	3.897
NM_146017	Gabrp	3.866
NM_010266	Gda	3.86
NM_011402	Slc34a2	3.857
NM_001012306	Hsd3b3	3.839
NM_007385	Apoc4	3.799
NM_001042613	Sepp1	3.798
NM_001161621	Aoc1	3.759
NM_008230	Hdc	3.741
NM_001285956	Podn	3.739
NM_017399	Fabp1	3.737
NM_025750	4933417A18Rik	3.724
NM_008059	G0s2	3.724
NM_001001446	Cyp2c44	3.716
NM_013786	Hsd17b6	3.684
NM_178711	Plscr4	3.657
NM_172500	Syne3	3.648
NM_001033158	Rasl12	3.644
NM_007815	Cyp2c29	3.643
NM_009369	Tgfbi	3.639
NM_009184	Ptk6	3.637
NM_133226	Pdzd3	3.629
NM_027132	Otop3	3.619
NM_031191	Prl2c2	3.604
NM_001104531	Cyp2d11	3.593
NM_173740	Maoa	3.592
NM_001122660	Gm10639	3.587
NM_079835	Btnl2	3.579
NM_009626	Adh7	3.578
NM_010005	Cyp2d10	3.564

NM_183224	Fam19a3	3.563
NM_138665	Sardh	3.552
NM_053200	Ces1d	3.533
NM_134005	Enpp3	3.514
NM_177388	Slc41a2	3.512
NM_207268	Ccdc87	3.506
NM_030747	Btnl6	3.503
NM_080437	Celsr3	3.501
NM_009999	Cyp2b10	3.486
NM_001205249	Gm9994	3.47
NM_001166063	Ccdc152	3.443
NM_001243092	Gm3776	3.442
NM_001039243	Erich4	3.418
NM_133217	Bco2	3.414
NM_001081032	Gm8909	3.398
NM_008182	Gsta2	3.397
NM_001099331	R3hdml	3.394
NM_019741	Slc2a5	3.394
NM_017474	Clca3	3.393
NM_009731	Akr1b7	3.392
NM_001145895	1700019G17Rik	3.388
NM_177450	Cndp1	3.384
NM_001029867	Ugt2b36	3.379
NM_153193	Hsd3b2	3.377
NM_001163472	Cyp2d22	3.375
NM_007819	Cyp3a13	3.373
NM_172715	Agpat9	3.366
NM_022816	Acot10	3.361
NM_001162880	Syce3	3.343
NM_027237	2010003K11Rik	3.342
NM_134246	Acot3	3.332
NM_027217	1810046K07Rik	3.326
NM_175512	Dhrs9	3.325
NM_130452	Bbox1	3.317
NM_008181	Gsta1	3.317
NM_177448	Mogat2	3.308
NM_029562	Cyp2d26	3.298
NM_023137	Ubd	3.286
NM_001033775	4933422H20Rik	3.284
NM_026947	Eci3	3.283
NM_019432	Tmem37	3.276
NM_001199967	Gm11127	3.273
NM_028341	Ttc39c	3.268
NM_011723	Xdh	3.268
NM_153506	Clec2e	3.267
NM_011978	Slc27a2	3.258
NM_023608	Gdpd2	3.248
NM_025831	Pxdc1	3.238
NM_001081082	Alpi	3.232
NM_009139	Ccl6	3.218
NM_001177542	C87977	3.215
NM_146230	Acaa1b	3.204
NM_001271402	Ephx2	3.187
NM_144903	Aldob	3.186
NM_009705	Arg2	3.182
NM_001085418	Pramel5	3.18
NM_001105245	Pcdh19	3.179
NM_001024719	Cyp2c67	3.176
NM_008199	H2-Bl	3.172
NM_007672	Cdr2	3.162
NM_001033199	AI747448	3.158
NM_001204333	Cyp4f14	3.155
NM_007823	Cyp4b1	3.154
NM_198171	Ces2b	3.151
NM_001145799	Ctla2a	3.143
NM_008630	Mt2	3.143
NM_001029984	Fcrlb	3.141

NM_001010834	Slc10a5	3.128
NM_011998	Chst4	3.126
NM_025453	Tm4sf20	3.12
NM_028077	1810055G02Rik	3.119
NM_009693	Apob	3.113
NM_001013785	Akr1c19	3.109
NM_008586	Mep1b	3.102
NM_008587	Mertk	3.102
NM_001285845	Paqr7	3.101
NM_008571	Mcpt2	3.099
NM_027391	Iyd	3.093
NM_019546	Prodh2	3.067
NM_134420	Slc26a6	3.056
NM_031197	Slc2a2	3.056
NM_001195596	Smlr1	3.049
NM_026819	Dhrs1	3.043
NM_008979	Ptpn22	3.038
NM_001033380	Itpripl2	3.025
NM_027066	Tmem89	3.019
NM_001025570	Prrx1	3.018
NM_145222	B3gnt7	3.016
NM_183160	Tmem252	3.011
NM_019580	Gde1	3.002
NM_013825	Ly75	2.993
NM_133969	Cyp4v3	2.982
NM_001081369	Ccdc153	2.978
NM_033314	Slco2a1	2.975
NM_009755	Bmp1	2.972
NM_145603	Ces2c	2.971
NM_020622	Fam3b	2.966
NM_001163457	Mttp	2.963
NM_001085390	Dusp5	2.961
NM_001163756	Ces2e	2.957
NM_001159738	Ccl20	2.948
NM_019792	Cyp3a25	2.946
NM_021353	Slc26a3	2.945
NM_028979	Cyp2j9	2.944
NM_001100181	Cyp4a32	2.924
NM_001039219	Gm6086	2.92
NM_175511	Fam78a	2.917
NM_011452	Serpinb9b	2.903
NM_023529	Ms4a10	2.901
NM_013743	Pdk4	2.891
NM_030084	Gpr108	2.884
NM_011122	Plod1	2.88
NM_026945	Adh6a	2.871
NM_011312	S100a5	2.865
NM_001289531	Cndp2	2.861
NM_010014	Dab1	2.86
NM_028176	Cda	2.856
NM_001113418	Ppara	2.853
NM_016908	Syt5	2.848
NM_001105160	Cyp3a59	2.847
NM_025274	Dppa5a	2.841
NM_019810	Slc5a1	2.838
NM_026967	Rhebl1	2.835
NM_010008	Cyp2j6	2.831
NM_029360	Tm4sf5	2.83
NM_019878	Sult1b1	2.825
NM_001160178	Klhdc7b	2.824
NM_173404	Bmp3	2.818
NM_001164562	Sec22c	2.818
NM_144544	2210407C18Rik	2.814
NM_027464	Fam213a	2.814
NM_153119	Plekho2	2.813
NM_009178	St3gal4	2.807
NM_026960	Gsdmd	2.803

NM_026384	Dgat2	2.789
NM_053217	2010002M12Rik	2.786
NM_008360	Il18	2.779
NM_139198	Plac8	2.766
NM_001201389	Gm11128	2.754
NM_172621	Clic5	2.752
NM_053096	Cml2	2.751
NM_017396	Cyp3a41a	2.749
NM_001111100	Lipa	2.744
NM_001080934	Slc16a5	2.735
NM_001033498	Gramd2	2.726
NM_001177467	Gm7030	2.717
NM_001081756	Nckap5	2.709
NM_008519	Ltb4r1	2.706
NM_009738	Bche	2.705
NM_009804	Cat	2.701
NM_001105252	Tmc5	2.679
NM_001253910	Gm4477	2.672
NM_031884	Abcg5	2.671
NM_139300	Mylk	2.658
NM_023835	Trim12a	2.657
NM_144878	Fmo4	2.656
NM_016771	Sult1d1	2.654
NM_001291152	Sgk2	2.651
NM_029870	Crebrf	2.649
NM_008013	Fgl2	2.643
NM_001160411	Gstm4	2.643
NM_001039586	Glyctk	2.641
NM_001252530	Slco2b1	2.64
NM_173019	Pfkfb4	2.637
NM_008439	Khk	2.625
NM_001199015	Slc7a9	2.609
NM_007763	Crip1	2.608
NM_027982	Ppm1j	2.604
NM_001167936	Zyg11a	2.589
NM_011105	Pkdrej	2.571
NM_026364	Prpsap1	2.563
NM_001286005	Abcg8	2.562
NM_001037842	Cml3	2.562
NM_010189	Fcgrt	2.56
NM_010004	Cyp2c40	2.559
NM_013921	Prss30	2.555
NM_134247	Acot4	2.554
NM_001005341	Ypel2	2.543
NM_175324	Acad11	2.542
NM_008842	Pim1	2.537
NM_001271898	Acox1	2.533
NM_001039555	Cyp2c68	2.533
NM_001011873	Xkr9	2.531
NM_028785	Dock8	2.528
NM_001251849	Ms4a18	2.527
NM_028094	Ugt2a3	2.519
NM_010358	Gstm1	2.517
NM_010658	Mafb	2.515
NM_025929	2010109I03Rik	2.504
NM_026907	Sectm1b	2.498
NM_199422	S100a7a	2.497
NM_018795	Abcc6	2.495
NM_001161837	Ptprr	2.495
NM_001160149	Cgref1	2.493
NM_013602	Mt1	2.487
NM_029875	Slc35e3	2.485
NM_016972	Slc7a8	2.473
NM_144520	Sec14l2	2.459
NM_001170643	Rnf144b	2.458
NM_011954	Prl2c4	2.451
NM_001005858	I830012O16Rik	2.447

NM_029595	Pbp2	2.445
NM_008585	Mep1a	2.443
NM_170778	Dpyd	2.441
NM_001190297	Gpr155	2.441
NM_134072	Akr1c14	2.437
NM_010392	H2-Q2	2.437
NM_153527	Dnajb13	2.434
NM_001081259	Mfsd7b	2.421
NM_011118	Prl2c3	2.42
NM_001167828	Trim30d	2.412
NM_030746	Btnl4	2.406
NM_207208	Clca6	2.406
NM_001163748	Pde9a	2.404
NM_178767	Agmo	2.401
NM_011989	Slc27a4	2.398
NM_133684	Marc2	2.394
NM_029555	Gstk1	2.389
NM_025510	Adprm	2.386
NM_001290273	Marc1	2.383
NM_001282993	Cobl	2.38
NM_001285881	D630023F18Rik	2.379
NM_145700	Ackr4	2.374
NM_026212	Agpat2	2.369
NM_133995	Upb1	2.368
NM_145532	Mall	2.361
NM_010173	Faah	2.36
NM_024442	Cyp4f16	2.357
NM_001033208	Myzap	2.354
NM_027950	Osgin1	2.352
NM_001122603	Fcgbp	2.35
NM_019975	Hacl1	2.345
NM_172133	Adap2	2.341
NM_001013028	Tmem263	2.34
NM_001123371	Pnp2	2.339
NM_007435	Abcd1	2.337
NM_029787	Cyb5r3	2.337
NM_001146007	Trim12c	2.337
NM_001081051	D130043K22Rik	2.329
NM_130864	Acaa1a	2.325
NM_024413	Plekhf1	2.323
NM_028236	Ceacam18	2.321
NM_153587	Rps6ka5	2.318
NM_019395	Fbp1	2.317
NM_028967	Batf2	2.31
NM_175474	Fam109a	2.309
NM_001172472	Sphk1	2.303
NM_027816	Cyp2u1	2.301
NM_001162425	Efna1	2.3
NM_001033879	Tubal3	2.295
NM_001294138	Gyk	2.292
NM_207270	Ptprh	2.292
NM_001109975	Synpo	2.292
NM_028955	4933427G17Rik	2.282
NM_001171003	Mgam	2.277
NM_008694	Ngp	2.276
NM_001252573	Slc35c2	2.274
NM_182805	Gpt	2.272
NM_023624	Lrat	2.27
NM_001037170	Tomm40l	2.268
NM_015790	Icosl	2.267
NM_019687	Slc22a4	2.258
NM_001146708	Fas	2.254
NM_025687	Tex12	2.254
NM_027909	C2cd2l	2.253
NM_001039137	Scoc	2.253
NM_009138	Ccl25	2.247
NM_009523	Wnt4	2.247

NM_001025577	Maf	2.237
NM_018744	Sema6a	2.236
NM_011920	Abcg2	2.235
NM_001293795	Tm6sf2	2.233
NM_177371	Tnfsf15	2.226
NM_007902	Edn2	2.225
NM_011731	Slc6a20b	2.224
NM_175408	Tmem139	2.223
NM_001159626	Hagh	2.218
NM_009789	S100g	2.217
NM_001146710	Ppp1r18	2.214
NM_172256	Dync2li1	2.21
NM_028832	Mterf2	2.202
NM_001199283	Slc43a2	2.202
NM_001111320	Idh1	2.196
NM_001291859	Rhoc	2.189
NM_001267695	Ctss	2.187
NM_001082483	Efr3b	2.187
NM_029494	Rab30	2.186
NM_001290733	Osbpl6	2.182
NM_145424	BC089597	2.181
NM_012030	Slc9a3r1	2.18
NM_028623	Cst6	2.179
NM_025429	Serpinb1a	2.179
NM_011327	Scp2	2.178
NM_175207	Ankrd9	2.175
NM_021454	Cdc42ep5	2.175
NM_145932	Slc51a	2.175
NM_001159986	Sec16b	2.172
NM_018779	Pde3a	2.17
NM_009475	Prap1	2.162
NM_027211	Anxa13	2.154
NM_133867	Eps8l3	2.148
NM_001039071	Ldb3	2.145
NM_177357	Kalrn	2.14
NM_001177696	Ablim2	2.133
NM_007519	Baat	2.132
NM_007576	C4bp	2.131
NM_146126	Sord	2.128
NM_007408	Plin2	2.126
NM_001083934	Myom1	2.123
NM_008670	Naip1	2.122
NM_001034898	Ms4a15	2.119
NM_010751	Mxd1	2.117
NM_001301295	Cidec	2.116
NM_001099917	Smim24	2.113
NM_011396	Slc22a5	2.106
NM_027853	Mettl7b	2.104
NM_174995	Mgst2	2.096
NM_001085385	1600014C10Rik	2.093
NM_013806	Abcc2	2.089
NM_026915	Lyzl4	2.088
NM_001112702	Tnni1	2.086
NM_178661	Creb3l2	2.083
NM_175132	Synpo2l	2.083
NM_197985	Adipor2	2.079
NM_001081219	Myo1a	2.073
NM_026328	Reg4	2.069
NM_133660	Ces1e	2.068
NM_001037932	Gm11437	2.067
NM_023113	Aspa	2.061
NM_010125	Elf5	2.058
NM_001101600	Gm7616	2.058
NM_001134391	Apobec1	2.056
NM_177470	Acaa2	2.051
NM_001162503	Sqrdl	2.051
NM_001277315	Fam134b	2.05

NM_001289791	Asic1	2.046
NM_010153	Erbb3	2.035
NM_001166065	Gcnt4	2.033
NM_172495	Ncoa7	2.028
NM_172428	Ccdc134	2.021
NM_001013607	Vmo1	2.021
NM_021411	Rab37	2.019
NM_001252443	Tfg	2.019
NM_178257	Il22ra1	2.016
NM_001190330	Ces2a	2.014
NM_175164	Arhgap26	2.012
NM_020581	Angptl4	2.011
NM_145419	Hkdc1	2.011
NM_001142959	Bcl2l15	2.008
NM_027077	1700016C15Rik	2.004
NM_010724	Psmb8	2.004
NM_028191	Cyp2c65	2.001
NM_026240	Gramd3	1.998
NM_026779	Mocos	1.991
NM_016800	Vti1b	1.988
NM_172541	Tmem120a	1.986
NM_001164640	Apol7a	1.979
NM_001114322	Cdhr5	1.979
NM_175507	Slc35g1	1.974
NM_010271	Gpd1	1.973
NM_153408	Neurl3	1.972
NM_007635	Ccng2	1.971
NM_018830	Asah2	1.967
NM_025341	Abhd6	1.966
NM_008278	Hpgd	1.964
NM_001170978	Abat	1.963
NM_021453	Pga5	1.963
NM_001011707	Cyp2c66	1.961
NM_001013780	Slc25a34	1.958
NM_175030	Tctex1d4	1.955
NM_030719	Gatsl2	1.949
NM_029662	Mfsd2a	1.947
NM_007381	Acadl	1.945
NM_026672	Gstm7	1.944
NM_001024619	Tsku	1.943
NM_010390	H2-Q1	1.939
NM_013807	Plk3	1.939
NM_001081310	Tmem236	1.939
NM_133350	Mapre3	1.931
NM_153056	Sirt7	1.925
NM_007437	Aldh3a2	1.922
NM_001159401	Upp1	1.922
NM_001177482	Gm14851	1.92
NM_013515	Stom	1.917
NM_177564	Dhrs11	1.916
NM_194344	Sh3tc1	1.916
NM_031181	Siglece	1.913
NM_010137	Epas1	1.911
NM_010753	Mxd4	1.91
NM_025590	Acot11	1.908
NM_027587	Micalcl	1.908
NM_001297612	Mylk3	1.904
NM_007467	Aplp1	1.901
NM_001159593	Slc20a1	1.9
NM_001081060	Slc9a3	1.897
NM_181325	Slc25a15	1.896
NM_011614	Tnfsf12	1.895
NM_011703	Vipr1	1.894
NM_177321	Mia2	1.886
NM_007553	Bmp2	1.885
NM_011756	Zfp36	1.885
NM_175305	Lrrc19	1.881

NM_023737	Ehhadh	1.878
NM_175133	Gucd1	1.875
NM_001253692	Elmod3	1.874
NM_024229	Pcyt2	1.873
NM_009113	S100a13	1.872
NM_013920	Hnf4g	1.868
NM_030018	Tmem50b	1.868
NM_010046	Dgat1	1.863
NM_001164359	Erlin1	1.861
NM_001004157	Scarf1	1.861
NM_010180	Fbln1	1.86
NM_013831	Pstpip2	1.858
NM_176954	Celf5	1.857
NM_001162414	Nlrp1b	1.857
NM_001287171	Sct	1.856
NM_001009949	Slc25a51	1.853
NM_001254747	Il15	1.85
NM_001163440	Mov10	1.85
NM_027558	Pgrmc2	1.845
NM_007760	Crat	1.843
NM_025535	Sar1b	1.841
NM_010301	Gna11	1.837
NM_144869	BC021614	1.831
NM_013867	Bcar3	1.831
NM_001291042	Tmem220	1.831
NM_029091	Klc4	1.83
NM_010637	Klf4	1.829
NM_010111	Efnb2	1.824
NM_022653	Thop1	1.824
NM_013571	Ksr1	1.823
NM_027839	Ceacam20	1.822
NM_001253353	Fam214b	1.82
NM_011032	P4hb	1.814
NM_001271005	C920025E04Rik	1.813
NM_146077	Trim31	1.813
NM_001161847	Sgk1	1.809
NM_007692	Chkb	1.807
NM_023154	Ethe1	1.804
NM_027227	Glod5	1.803
NM_027491	Rragd	1.803
NM_001039515	Arl4a	1.801
NM_018824	Slc23a2	1.798
NM_134122	Nrm	1.797
NM_133918	Emilin1	1.794
NM_001164804	Coro2a	1.791
NM_001288627	Emp1	1.789
NM_178669	Clrn3	1.784
NM_010359	Gstm3	1.783
NM_021542	Kcnk5	1.783
NM_001199118	Lpin3	1.783
NM_023383	Aadac	1.782
NM_198604	Plekhg6	1.782
NM_027913	Vwce	1.777
NM_207205	Igsf3	1.776
NM_001290508	Dolpp1	1.772
NM_025661	Ormdl3	1.772
NM_001168577	Nat2	1.77
NM_010484	Slc6a4	1.769
NM_001177439	Tldc2	1.769
NM_016752	Slc35b1	1.768
NM_001145875	Adtrp	1.767
NM_001190448	Ddc	1.767
NM_011517	Sycp3	1.767
NM_001122594	Phlpp2	1.766
NM_019875	Abcb9	1.764
NM_008208	H2-T3	1.763
NM_144797	Metrnl	1.762

NM_009205	Slc3a1	1.762
NM_001135100	Il34	1.761
NM_178595	Ptrh1	1.76
NM_001253796	Smim22	1.76
NM_173370	Cds1	1.759
NM_001146330	Gpr52	1.756
NM_001081656	Neurl1b	1.756
NM_023530	Pla2g12b	1.755
NM_001271496	Chka	1.754
NM_145934	Stap2	1.753
NM_011636	Plscr1	1.749
NM_134020	Tmed4	1.748
NM_011609	Tnfrsf1a	1.748
NM_029035	Spsb1	1.746
NM_008512	Lrp1	1.745
NM_020520	Slc25a20	1.745
NM_026740	Slc46a1	1.745
NM_001290826	Cpeb3	1.741
NM_001013022	Odf3b	1.738
NM_177366	Gpr157	1.734
NM_130869	Nobox	1.731
NM_001163028	Bco1	1.73
NM_001134829	Lpgat1	1.729
NM_001004178	AA415398	1.728
NM_177382	Cyp2r1	1.728
NM_178035	Fads6	1.728
NM_146004	Mfsd6l	1.727
NM_010398	H2-T23	1.725
NM_145962	Pank3	1.725
NM_033371	Ppp1r16a	1.725
NM_172145	Eva1b	1.724
NM_020490	Ltb4r2	1.724
NM_207242	Npc1l1	1.724
NM_026436	Tmem86a	1.724
NM_001276764	Dst	1.721
NM_201643	Ugt1a5	1.721
NM_001164655	9530053A07Rik	1.72
NM_023160	Cml1	1.72
NM_153782	Fam20a	1.716
NM_173038	Tbcel	1.715
NM_198653	Iars2	1.714
NM_001083884	Lypd8	1.713
NM_138587	Fam3c	1.712
NM_010501	Ifit3	1.712
NM_025582	Fam213b	1.71
NM_007480	Arf5	1.708
NM_009894	Cideb	1.706
NM_201641	Ugt1a10	1.701
NM_201644	Ugt1a9	1.701
NM_053085	Tcf23	1.698
NM_021534	Pxmp4	1.695
NM_153537	Phldb1	1.693
NM_022430	Ms4a8a	1.692
NM_008769	Otc	1.692
NM_145079	Ugt1a6a	1.691
NM_028085	Anks4b	1.69
NM_026701	Pbld1	1.688
NM_001146690	Chpt1	1.685
NM_010357	Gsta4	1.685
NM_001014399	Abi3bp	1.681
NM_001033966	Ak2	1.681
NM_201410	Ugt1a6b	1.68
NM_010959	Oit3	1.676
NM_007485	Rhod	1.672
NM_001013751	Syna	1.671
NM_028998	Themis3	1.667
NM_177152	Lrig3	1.666

NM_007620	Cbr1	1.665
NM_175092	Rhof	1.665
NM_001001321	Slc35d2	1.662
NM_001033364	Cdhr2	1.66
NM_009444	Tgoln2	1.659
NM_021451	Pmaip1	1.658
NM_153574	Fam13a	1.657
NM_001142809	Slc6a8	1.657
NM_201642	Ugt1a7c	1.657
NM_029840	Tstd3	1.65
NM_201645	Ugt1a1	1.65
NM_011596	Atp6v0a2	1.647
NM_001162533	Sh3d21	1.646
NM_175180	Wdr44	1.646
NM_013632	Pnp	1.645
NM_010726	Phyh	1.644
NM_013701	Ugt1a2	1.643
NM_011227	Rab20	1.633
NM_011575	Tff3	1.633
NM_031250	Ucn3	1.632
NM_029858	Ston1	1.63
NM_016892	Ccs	1.628
NM_026085	Pbld2	1.628
NM_010016	Cd55	1.627
NM_001290837	Serf2	1.623
NM_001163144	Pcsk5	1.622
NM_009288	Stk10	1.622
NM_023322	Zkscan14	1.621
NM_025558	Cyb5b	1.619
NM_011469	Sprr2b	1.617
NM_027166	Ypel5	1.617
NM_001037741	Gpx4	1.616
NM_001039507	Lipe	1.612
NM_009620	Adam4	1.61
NM_177171	Heatr5a	1.609
NM_053262	Hsd17b11	1.609
NM_001253813	Ano6	1.606
NM_133898	N4bp2l1	1.606
NM_173047	Cbr3	1.604
NM_001083894	Liph	1.603
NM_001048008	Agtpbp1	1.601
NM_016811	Dgka	1.601
NM_153140	Rab11fip3	1.596
NM_001033286	Slc30a10	1.596
NM_001159627	Heph	1.595
NM_016720	Neu3	1.592
NM_032002	Nrg4	1.592
NM_011051	Pdcd6	1.592
NM_001114332	Slc16a10	1.592
NM_026316	Aldh3b1	1.59
NM_145496	Dak	1.59
NM_153054	Slc18a1	1.589
NM_133683	Tmem19	1.587
NM_001195084	Plscr2	1.586
NM_001164724	Il33	1.579
NM_009735	B2m	1.573
NM_026680	Golt1a	1.573
NM_026667	Fam114a1	1.571
NM_001177621	Slc5a6	1.569
NM_197990	1700025G04Rik	1.566
NM_026346	Fbxo32	1.564
NM_028102	Ddhd2	1.563
NM_026169	Frmd8	1.562
NM_053116	Wnt16	1.561
NM_001193305	Mical2	1.56
NM_001290563	Ttc16	1.56
NM_080435	Adcy4	1.558

NM_001085509	Myom3	1.557
NM_001083906	Nr3c2	1.556
NM_011850	Nr0b2	1.552
NM_001290570	Ralgps1	1.552
NM_013541	Gstp1	1.549
NM_001287817	Fmn1	1.547
NM_001159393	Irf1	1.547
NM_026814	Ppp1r27	1.545
NM_011923	Angptl2	1.544
NM_001039494	Tex40	1.544
NM_009443	Tgoln1	1.544
NM_007994	Fbp2	1.543
NM_010739	Muc13	1.543
NM_199011	Dgkq	1.542
NM_001012363	Slc2a9	1.541
NM_025951	Pi4k2b	1.539
NM_009427	Tob1	1.537
NM_144830	Tmem106a	1.536
NM_133888	Smpdl3b	1.535
NM_001290568	Ift74	1.533
NM_001291000	Sema6d	1.533
NM_010489	Hyal2	1.531
NM_001039530	Parp14	1.53
NM_009177	St3gal1	1.529
NM_008292	Hsd17b4	1.526
NM_183178	Fsd1	1.525
NM_008212	Hadh	1.525
NM_001141948	Nmi	1.525
NM_001171034	Tmbim6	1.525
NM_029643	Slc52a2	1.523
NM_001113417	Thrb	1.523
NM_001014390	Dyrk2	1.521
NM_001033778	Gm5535	1.517
NM_145829	Nags	1.517
NM_007885	Slc26a2	1.517
NM_023668	Ndel1	1.513
NM_008706	Nqo1	1.511
NM_001033270	Slc4a7	1.511
NM_133753	Errfi1	1.509
NM_029044	Lrrc48	1.507
NM_013565	Itga3	1.506
NM_199257	Tpte	1.506
NM_025797	Cyb5a	1.504
NM_011937	Gnpda1	1.504
NM_001113460	Tec	1.504
NM_025569	Mgst3	1.501
NM_001034097	Tnfsf12Tnfsf13	1.5
NM_145505	Fam160b1	1.498
NM_172612	Rnd1	1.498
NM_133967	Zdhhc7	1.495
NM_025295	Btd	1.494
NM_001003917	Atg9a	1.492
NM_008688	Nfic	1.491
NM_177016	Slc17a4	1.491
NM_019936	Cript	1.49
NM_134130	Abhd3	1.488
NM_026963	Lzic	1.488
NM_023138	Map2k2	1.488
NM_026268	Dusp6	1.487
NM_001286217	Fuom	1.487
NM_001164117	Serpinb6a	1.487
NM_031252	Il23a	1.486
NM_001039677	Slc30a2	1.486
NM_001033235	Trim40	1.486
NM_181547	Nostrin	1.485
NM_001177360	Gpr137	1.483
NM_027976	Acsl5	1.481

NM_001267724	Asb13	1.481
NM_019980	Litaf	1.48
NM_178692	C130074G19Rik	1.479
NM_183173	Sowaha	1.479
NM_008486	Anpep	1.473
NM_001114595	Ehbp1l1	1.471
NM_028713	Rftn2	1.471
NM_177130	Glt28d2	1.469
NM_054095	Necab2	1.469
NM_008338	Ifngr2	1.468
NM_007533	Bckdha	1.467
NM_025834	Proz	1.467
NM_001146001	Pdzk1	1.466
NM_016907	Spint1	1.466
NM_001164565	Acnat1	1.465
NM_010947	Ntn3	1.465
NM_001039092	Tom1l2	1.465
NM_023733	Crot	1.463
NM_181729	Muc6	1.463
NM_001281472	Psme2b	1.463
NM_183116	Slc18b1	1.461
NM_001083958	Zfp655	1.46
NM_153069	Leap2	1.458
NM_028787	Slc35f5	1.458
NM_010795	Mgat3	1.457
NM_001204931	Reep6	1.457
NM_030004	Cryl1	1.456
NM_008184	Gstm6	1.455
NM_001039959	Ahnak	1.454
NM_027196	Pold4	1.454
NM_010870	Naip5	1.453
NM_028943	Sgms2	1.453
NM_001289487	Exoc3l4	1.452
NM_001160368	Rnf152	1.452
NM_153789	Mylip	1.451
NM_133191	Eps8l2	1.45
NM_008621	Mpp1	1.45
NM_146149	Fam151a	1.449
NM_018811	Abhd2	1.448
NM_001039466	Trim46	1.445
NM_010757	Mafk	1.442
NM_021409	Pard6b	1.442
NM_001164606	Ccdc116	1.441
NM_001029929	Zmynd15	1.441
NM_207677	Dedd2	1.44
NM_025519	Chmp4c	1.439
NM_001130458	Tcn2	1.439
NM_025988	Acbd4	1.438
NM_001159543	Dpp4	1.437
NM_181848	Optn	1.437
NM_054088	Pnpla3	1.437
NM_001159394	Nfkbiz	1.436
NM_001163159	Pcyt1a	1.435
NM_001253736	Pdlim2	1.435
NM_029031	Shpk	1.434
NM_001163687	Naaa	1.433
NM_001290481	Rxra	1.432
NM_194348	Atg2a	1.431
NM_001291004	H6pd	1.431
NM_008681	Ndrg1	1.428
NM_029310	Fabp12	1.427
NM_146125	Itpka	1.427
NM_053109	Clec2d	1.426
NM_153557	BC029214	1.425
NM_007670	Cdkn2b	1.425
NM_026159	Retsat	1.425
NM_145986	Fam83f	1.423

NM_001026214	Entpd5	1.422
NM_028292	Ppme1	1.422
NM_019979	Selk	1.421
NM_012001	Cops4	1.42
NM_008795	Cdk18	1.417
NM_153121	Lysmd1	1.417
NM_011946	Map3k2	1.416
NM_145535	Sdcbp2	1.416
NM_009142	Cx3cl1	1.415
NM_009504	Vdr	1.414
NM_008349	Il10rb	1.413
NM_025653	3110001I22Rik	1.412
NM_011913	Best1	1.412
NM_001025371	Serinc4	1.412
NM_133215	Mtmr4	1.411
NM_021524	Nampt	1.411
NM_001145644	Phgr1	1.411
NM_175244	Hectd3	1.41
NM_025347	Ypel3	1.41
NM_008618	Mdh1	1.409
NM_008617	Mdh2	1.409
NM_028493	Rhobtb3	1.409
NM_027184	Ipmk	1.407
NM_001161548	Tmem184a	1.406
NM_025785	Fbxo25	1.404
NM_001290643	Rp2h	1.401
NM_025572	2610528J11Rik	1.4
NM_001190322	Chchd7	1.399
NM_001101431	Mkrn2os	1.399
NM_001110201	Yif1b	1.399
NM_001253783	Def8	1.398
NM_026700	Dopey2	1.398
NM_015822	Fbxl3	1.398
NM_001290796	Ppp1r14d	1.398
NM_008508	Lor	1.397
NM_023402	Myl12b	1.397
NM_153550	Dirc2	1.396
NM_027715	Otud1	1.396
NM_033269	Chrm3	1.395
NM_013518	Fgf9	1.395
NM_001099779	Pklr	1.395
NM_009228	Snta1	1.395
NM_001045515	Synj1	1.395
NM_001101605	Gm14446	1.394
NM_001047159	Net1	1.393
NM_026331	Slc25a37	1.392
NM_012014	Gprin1	1.391
NM_199310	Ccdc32	1.39
NM_172893	Parp12	1.39
NM_001042659	Fzd5	1.389
NM_201529	Lmo7	1.389
NM_009466	Ugdh	1.387
NM_009897	Ckmt1	1.385
NM_009948	Cpt1b	1.385
NM_023480	Fahd1	1.384
NM_019993	Aldh9a1	1.383
NM_011673	Ugcg	1.383
NM_021539	Wsb2	1.382
NM_177263	Zhx3	1.38
NM_001291076	Snph	1.379
NM_025292	Synj2bp	1.378
NM_001159725	Rab17	1.377
NM_144803	Chrna2	1.376
NM_009949	Cpt2	1.375
NM_177662	Ctso	1.375
NM_001045536	Zzef1	1.374
NM_008247	Ppap2a	1.372

NM_001170911	Prr13	1.372
NR_122039	Tsc22d3	1.372
NM_001033231	Fam195b	1.371
NM_001001892	H2-K1	1.364
NM_028369	Mon1a	1.364
NM_001243062	Nr1i3	1.364
NM_001162416	Pfkfb2	1.364
NM_027788	Fam83c	1.363
NM_176963	Galm	1.362
NM_001291211	Pcmtd2	1.361
NM_011068	Pex11a	1.361
NM_017465	Sult2b1	1.361
NM_145421	Abhd17a	1.36
NM_008391	Irf2	1.36
NM_025619	1700019L03Rik	1.359
NM_029250	Etnk1	1.359
NM_008471	Krt19	1.359
NM_021882	Pmel	1.359
NM_001033367	Nlrc4	1.357
NM_175256	Heg1	1.356
NM_018810	Mkrn1	1.356
NM_001048177	Jak2	1.352
NM_024188	Oxct1	1.352
NM_012000	Cln8	1.351
NM_010170	F2rl2	1.351
NM_001253781	Prlr	1.351
NM_183285	Kctd2	1.35
NM_001177550	Zfp442	1.35
NM_001081074	A1cf	1.347
NM_010239	Fth1	1.346
NM_022889	Pes1	1.346
NM_025445	Arfgap3	1.345
NM_007865	Dll1	1.344
NM_008190	Guca2a	1.344
NM_001136075	Numb	1.343
NM_001290180	Nudt7	1.342
NM_013585	Psmb9	1.339
NM_133185	Rogdi	1.338
NM_001253679	Slc7a7	1.338
NM_016669	Crym	1.337
NM_008124	Gjb1	1.336
NM_001163239	Nqo2	1.335
NM_146050	Oit1	1.335
NM_011104	Prkce	1.334
NM_001177691	Gal3st1	1.333
NM_007611	Casp7	1.332
NM_021719	Cldn15	1.331
NM_016867	Gipc2	1.329
NM_026192	Calcoco1	1.328
NM_026251	Patl2	1.328
NM_030692	Sacm1l	1.326
NM_001145978	Parp4	1.325
NM_001163540	Plec	1.325
NM_011794	Bpnt1	1.324
NM_001081212	Irs2	1.324
NM_026494	Ppcs	1.323
NM_175308	Mob3c	1.322
NM_198168	Ppp2r5b	1.32
NM_001013370	Sesn1	1.318
NM_146260	Tmie	1.316
NM_029436	Klhl24	1.315
NM_009147	Sec23a	1.314
NM_026559	Txndc17	1.313
NM_001033156	Fbxo33	1.312
NM_133796	Arhgdia	1.31
NM_001177886	Igsf5	1.31
NM_146227	Prss50	1.31

NM_145539	Tm4sf4	1.31
NM_029688	Srxn1	1.309
NM_010902	Nfe2l2	1.303
NM_016808	Usp2	1.303
NM_001170855	Trim36	1.301
NM_177667	Ttc22	1.3
NM_001174169	Adora3	1.299
NM_001162947	Nek3	1.299
NM_001291061	Bfsp1	1.297
NM_010391	H2-Q10	1.294
NM_001290785	Sec24a	1.294
NM_172450	4930539E08Rik	1.293
NM_029901	Akr1c21	1.292
NM_177766	Slc35e1	1.292
NM_011342	Sec22b	1.291
NM_001139520	Samhd1	1.288
NM_009579	Slc30a1	1.288
NM_025706	Tbc1d15	1.286
NM_146151	Tesk2	1.285
NM_027919	Tha1	1.284
NM_172546	Cnksr3	1.283
NM_007707	Socs3	1.282
NM_183112	1700029I15Rik	1.28
NM_001103177	Ablim1	1.28
NM_008898	Por	1.279
NM_026924	Ovol2	1.277
NM_027135	Sec24d	1.277
NM_172723	Adap1	1.276
NM_001290676	Cpeb4	1.276
NM_178623	Urgcp	1.276
NM_030257	Lysmd3	1.275
NM_009811	Casp6	1.274
NM_001289554	Styxl1	1.274
NM_019585	Espn	1.271
NM_001162410	Chuk	1.268
NM_021537	Stk25	1.268
NM_197986	Tmem140	1.268
NM_013778	Akr1c13	1.267
NM_173440	Nrip1	1.266
NM_001080742	Vamp5	1.265
NM_183137	Enthd2	1.264
NM_001290475	Tdrd7	1.264
NM_001163504	Nr1h4	1.261
NM_001159525	Pex19	1.261
NM_013495	Cpt1a	1.26
NM_027998	Cldn23	1.259
NM_177567	BC049762	1.258
NM_018864	Impa1	1.258
NM_001190264	Mrps36	1.258
NM_026073	Ift22	1.256
NM_024190	Chmp1b	1.255
NM_001172424	Dhrs3	1.255
NM_001145884	Itgb5	1.255
NM_177412	Tmcc1	1.255
NM_027711	Iqgap2	1.254
NM_008991	Abcd3	1.252
NM_008119	Gip	1.252
NM_001033210	Pls1	1.249
NM_021519	Edf1	1.247
NM_010473	Hrc	1.247
NM_001001495	Tnip3	1.247
NM_001136055	Cd82	1.244
NM_172404	Ccbl1	1.243
NM_028900	Gcc1	1.243
NM_001291186	Abr	1.242
NM_015791	Fbxo8	1.242
NM_001168471	Dynll2	1.241

NM_010568	Insr	1.241
NM_020042	Mocs1	1.241
NM_007393	Actb	1.24
NM_030717	Lactb	1.239
NM_001134692	Ost4	1.237
NM_001083318	Etv3	1.236
NM_010380	H2-D1	1.236
NM_022305	B4galt1	1.234
NM_008185	Gstt1	1.234
NM_008306	Ndst1	1.234
NM_011882	Rnasel	1.234
NM_178656	Pirt	1.233
NM_198884	B4galnt3	1.232
NM_023158	Cxcl16	1.232
NM_027413	Lrrc28	1.229
NM_001177945	Aamdc	1.226
NM_001173500	G630090E17Rik	1.226
NM_178613	Gskip	1.226
NM_026497	Nudt12	1.224
NM_145401	Prkag2	1.224
NM_133902	Sdsl	1.224
NM_016794	Vamp8	1.224
NM_133240	Acot8	1.223
NM_007511	Atp7b	1.222
NM_013783	Mmel1	1.222
NM_025461	Cox16	1.218
NM_027828	Fam110c	1.218
NM_001290457	Relb	1.218
NM_011976	Sema4g	1.218
NM_001110218	Ppm1h	1.217
NM_026438	Ppa1	1.216
NM_183154	Zfyve1	1.216
NM_182994	Arl5a	1.214
NM_001033243	Ccdc114	1.214
NM_001285940	Fez2	1.212
NM_007563	Bpgm	1.211
NM_007388	Acp5	1.21
NM_144804	Depdc7	1.21
NM_001267808	H2-L	1.208
NM_001102436	Acbd5	1.207
NM_172685	Slc25a24	1.207
NM_027045	Ccser2	1.206
NM_153526	Insig1	1.206
NM_010500	Ier5	1.203
NM_001142411	Zfp937	1.203
NM_172825	Gpr128	1.202
NM_009748	Bet1	1.2
NM_029098	Lmbr1l	1.2
NM_001127318	Gucy2c	1.197
NM_181796	Gstp2	1.196
NM_030595	Nbea	1.196
NM_170756	Spata2	1.196
NM_145432	Heatr6	1.194
NM_007459	Ap2a2	1.192
NM_026403	Nop9	1.192
NM_001162970	Aim1l	1.191
NM_026283	Samd8	1.191
NM_029153	Scamp1	1.191
NM_025451	Camk2n1	1.188
NM_001177379	Cpeb2	1.185
NM_001170638	Slc17a1	1.185
NM_011671	Ucp2	1.185
NM_022996	Ndfip1	1.184
NM_001164361	Plekha8	1.184
NM_011399	Slc25a17	1.184
NM_176837	Arhgap18	1.183
NM_001033453	Pdp1	1.183

NM_025304	Lcmt1	1.182
NM_013790	Abcc5	1.181
NM_178693	Coq4	1.181
NM_028049	Fbxo22	1.181
NM_011660	Txn1	1.181
NM_001285517	Nr1h2	1.18
NM_001081151	Gan	1.178
NM_001034962	Sorbs1	1.176
NM_019935	Ovol1	1.175
NM_178931	Tnfrsf14	1.174
NM_133667	Pdk2	1.173
NM_145611	Kank2	1.172
NM_011932	Dapp1	1.17
NM_013754	Insl6	1.17
NM_001014981	Wdr7	1.17
NM_001113562	Cutc	1.168
NM_025841	Kdelr2	1.168
NM_145944	Ccdc25	1.167
NM_001081066	Dennd3	1.167
NM_001042592	Arrdc4	1.166
NM_010418	Herc2	1.166
NM_133664	Lad1	1.166
NM_130882	Cyp4f13	1.165
NM_029974	Dcst1	1.165
NM_025324	Zfp524	1.165
NM_016974	Dbp	1.164
NM_001162365	Ptk2b	1.164
NM_133722	Abhd17c	1.162
NM_001252450	Cldn25	1.161
NM_145130	Lpcat3	1.161
NM_001284409	Casp3	1.16
NM_030024	Prr15	1.158
NM_019551	Tdp2	1.158
NM_199306	Wdtc1	1.158
NM_007981	Acsl1	1.157
NM_001164564	Egfl7	1.156
NM_008105	Gcnt2	1.156
NM_021793	Tmem8	1.156
NM_028087	Gcnt3	1.155
NM_026254	Tbc1d23	1.155
NM_009790	Calm1	1.154
NM_025926	Dnajb4	1.154
NM_001042760	Slc22a18	1.154
NM_145987	Tmem82	1.154
NM_001039079	Prkcz	1.153
NM_032460	Gpank1	1.152
NM_007859	Dffb	1.151
NM_145449	Ifi27l2b	1.151
NM_153287	Csrnp1	1.15
NM_010688	Lasp1	1.15
NM_008926	Prkg2	1.15
NM_001166067	Slc4a5	1.15
NM_016852	Wbp2	1.15
NM_011189	Psme1	1.148
NM_001112744	Arhgef16	1.146
NM_001204904	4930558K02Rik	1.145
NM_026164	Pnpla8	1.145
NM_027840	Snx20	1.145
NM_001081490	Fbxo9	1.144
NM_025531	Slmo2	1.144
NM_010707	Lgals6	1.141
NM_139295	Mcfd2	1.14
NM_027872	Slc46a3	1.139
NM_001122640	Arhgap17	1.138
NM_001081047	Cnksr1	1.138
NM_007464	Birc3	1.137
NM_001290660	Cd302	1.137

NM_028521	Phospho2	1.137
NM_175212	Tmem65	1.137
NM_013850	Abca7	1.136
NM_001160180	Tor1aip2	1.136
NM_007808	Cycs	1.135
NM_001172561	Sphk2	1.135
NM_009900	Clcn2	1.134
NM_001282443	Mroh6	1.133
NM_178589	Tnfrsf21	1.132
NM_001206335	Itfg3	1.131
NM_030218	Misp	1.13
NM_172413	Rap2c	1.13
NM_024288	Rmnd5a	1.13
NM_001290769	Sqstm1	1.13
NM_008562	Mcl1	1.129
NM_145122	Pex16	1.129
NM_025729	Tab3	1.129
NM_008820	Pepd	1.127
NM_001254754	Echdc2	1.126
NM_011803	Klf6	1.125
NM_010706	Lgals4	1.125
NM_001025600	Cadm1	1.124
NM_025836	Plin3	1.124
NM_001081168	Sap30l	1.124
NM_173751	Ilvbl	1.123
NM_008410	Itm2b	1.123
NM_001290801	Mgat4a	1.123
NM_019966	Mlycd	1.123
NM_001242407	Fam73b	1.121
NM_009729	Atp6v0c	1.12
NM_008227	Hcn3	1.118
NM_177192	Dennd5b	1.117
NM_001033178	Tmem181a	1.117
NM_009807	Casp1	1.115
NM_001145800	Igsf9	1.114
NM_009163	Sgpl1	1.114
NM_001199203	Spag9	1.113
NM_010415	Hbegf	1.112
NM_001033382	Cacna2d4	1.111
NM_001142792	Tmem150b	1.11
NM_001190989	Ndfip2	1.109
NM_001025444	Aptx	1.108
NM_011512	Surf4	1.106
NM_016916	Blcap	1.105
NM_009509	Vil1	1.105
NM_001252582	Zfp410	1.105
NM_001291031	Ap5s1	1.104
NM_023248	Sbds	1.104
NM_001163847	Tbc1d24	1.104
NM_026880	Pink1	1.102
NM_199449	Zhx2	1.102
NM_001171000	Ahcyl2	1.101
NM_144900	Atp1a1	1.101
NM_009510	Ezr	1.101
NM_001101588	Cyp4f40	1.1
NM_026367	Gpatch2	1.1
NM_029649	Tmem101	1.1
NM_011076	Abcb1a	1.099
NM_001164735	Crlf2	1.099
NM_177718	Mb21d2	1.099
NM_001144992	2810459M11Rik	1.097
NM_138953	Ell2	1.096
NM_008453	Klf3	1.093
NM_001040087	Sytl2	1.093
NM_145443	L2hgdh	1.092
NM_001017985	C2cd3	1.091
NM_019680	Elf4	1.091

NM_001277932	Casp9	1.09
NM_194335	Naif1	1.09
NM_172476	Tmc7	1.09
NM_145925	Pttg1ip	1.089
NM_001163622	Prepl	1.088
NM_023580	Epha1	1.086
NM_022882	Lpin2	1.086
NM_010799	Minpp1	1.085
NM_001252473	Tjap1	1.084
NM_008971	Twf1	1.084
NM_030251	Abtb1	1.083
NM_026229	Gpr89	1.083
NM_008452	Klf2	1.083
NM_146025	Samd14	1.083
NM_016783	Pgrmc1	1.082
NM_172785	Zc3h12d	1.082
NM_001033759	Tmem2	1.081
NM_001146323	Hps3	1.08
NM_007661	Cdk11b	1.079
NM_197996	Tspan15	1.078
NM_029926	Irak4	1.077
NM_001128170	Cyld	1.076
NM_001252220	Nbr1	1.076
NM_001113553	Irak2	1.075
NM_025400	Nat9	1.075
NM_001291865	Sat1	1.075
NM_001033161	Tradd	1.075
NM_001081169	Aspg	1.074
NM_025816	Tax1bp1	1.074
NM_019793	Tspan3	1.074
NM_010579	Eif6	1.073
NM_010360	Gstm5	1.073
NM_001290797	Inpp4a	1.073
NM_025700	Pgm1	1.072
NM_028142	Nsun4	1.071
NM_177790	Zfp385c	1.071
NM_008102	Gch1	1.07
NM_001033225	Pnrc1	1.07
NM_008211	H3f3b	1.069
NM_175286	Tprn	1.069
NM_001026212	Ensa	1.068
NM_008928	Map2k3	1.068
NM_001033394	Tmem88b	1.068
NM_010511	Ifngr1	1.067
NM_001025208	LOC547349	1.067
NM_026772	Cdc42ep2	1.066
NM_009543	Rnf103	1.066
NM_029432	4930402H24Rik	1.065
NM_133674	Arhgef5	1.065
NM_009120	Sar1a	1.065
NM_198101	Gmip	1.064
NM_001159908	Zfand2a	1.064
NM_001159544	Frk	1.063
NM_028149	Fbxl20	1.062
NM_001110498	Ifnar2	1.062
NM_001145953	Lgals3	1.062
NM_023663	Ripk4	1.062
NM_001290993	Slc30a4	1.062
NM_027250	Coa7	1.06
NM_007456	Ap1m1	1.058
NM_028639	Ttc7	1.058
NM_001282064	Cyb561a3	1.057
NM_029857	Tmco4	1.057
NM_145434	Nr1d1	1.056
NM_178775	Rps6kc1	1.056
NM_021446	0610007P14Rik	1.055
NM_026969	Sec31a	1.055

NM_001271538	Myh14	1.054
NM_153405	Rbm45	1.053
NM_011542	Tcea3	1.053
NM_009320	Slc6a6	1.052
NM_018816	Apom	1.05
NM_001159344	Casz1	1.05
NM_145156	Slc25a28	1.048
NM_001098404	Nr1i2	1.047
NM_001253807	Ywhaz	1.047
NM_026373	Cdk2ap2	1.046
NM_001040026	Sco1	1.046
NM_024473	BC005537	1.045
NM_001145820	Gpd2	1.045
NM_001039536	Pigl	1.044
NM_001008700	Il4ra	1.043
NM_175423	Orai1	1.043
NM_172269	Vps18	1.042
NM_009730	Atrn	1.041
NM_001146010	Fchsd2	1.041
NM_001159367	Per1	1.04
NM_001127382	Rbm47	1.04
NM_178644	Oaf	1.039
NM_001252645	4833439L19Rik	1.038
NM_178878	Hadha	1.038
NM_008910	Ppm1a	1.038
NM_028029	Dnmbp	1.037
NM_019753	Cdh17	1.036
NM_001252282	Ogdh	1.036
NM_001163663	Rab6a	1.036
NM_001291835	Alas1	1.035
NM_181588	Cmbl	1.035
NM_026272	Narf	1.035
NM_001083334	Bin1	1.034
NM_019821	Gltp	1.033
NM_001130456	Sema6b	1.033
NM_178111	Trp53inp2	1.032
NM_026234	Pigm	1.031
NM_145441	Ubxn2a	1.03
NM_010307	Gnal	1.029
NM_153139	Slc36a1	1.029
NM_024257	Hdhd3	1.026
NM_027652	Ept1	1.025
NM_033477	D17H6S53E	1.024
NM_172821	Map3k13	1.024
NM_174989	Ticam1	1.024
NM_001290792	Wdr45	1.023
NM_181593	Itpkc	1.021
NM_009072	Rock2	1.02
NM_172698	Efcab14	1.018
NM_023324	Peli1	1.018
NM_001272090	Tysnd1	1.018
NM_001081232	D5Ertd579e	1.017
NM_001290558	Slc25a25	1.017
NM_133668	Slc25a3	1.017
NR_027704	Svip	1.017
NM_175105	Aqp11	1.015
NM_018859	Akr1e1	1.014
NM_001081109	Lmtk2	1.014
NM_001081549	Rcan1	1.014
NM_009351	Tep1	1.014
NM_001005247	Hps5	1.013
NM_177608	Secisbp2l	1.013
NM_023738	Uba7	1.013
NM_001037999	Dbi	1.012
NM_133990	Il13ra1	1.012
NM_152800	Tor2a	1.012
NM_001163695	4932438H23Rik	1.011

NM_053103	Entpd7	1.011
NM_011269	Rhag	1.011
NM_011486	Stat3	1.01
NM_019829	Stx5a	1.01
NM_022985	Zfand6	1.01
NM_175134	Ankrd46	1.009
NM_001256081	Myo7a	1.007
NM_001038625	Sertad2	1.007
NM_001285435	Adamtsl5	1.005
NM_010234	Fos	1.005
NM_001033259	Mcu	1.005
NM_134076	Abhd4	1.004
NM_001252454	Epn1	1.004
NM_008996	Rab1	1.003
NM_001101598	Isoc2a	1.002
NM_001042534	Capg	1.001
NM_001163780	Ick	1.001
NM_001177730	Nr1h3	1.001
NM_001033136	Rmdn3	1.001
NM_026617	Tmbim4	1.001

SUPPLEMENTAL MATERIALS AND METHODS

GRO-Seq data analysis

The quality of reads was confirmed using FastQC tool [1] and poor quality reads were removed (minimum 97% of bp over phred quality cutoff 10) using the FastX toolkit (http://hannonlab.cshl.edu/fastx_toolkit/). The filtered data was mapped using Bowtie [2] allowing up to two mismatches and reporting only one alignment for each read. Data analysis was performed using HOMER 4.3 [3].

HOMER programs "analyseRepeats.pl" and "getDiffExpression.pl" with the parameter "-batch" were used to get a list of differentially transcribed genes in the WENRC and ENRI samples while treating them as biological replicates utilizing edgeR [4]. Normalized values were used, denoted as RPKM (= reads per kilobase per million mapped reads = [# of mapped reads]/[length of transcript in kilo base]/[million mapped reads]). Differential transcripts were selected when RPKM > 0.5 in any sample, $\log_2$ fold change $\geq \pm 1$ between WENRC and ENRI and $P < 0.05$.

ChIP-Seq data analysis

Quality control analysis was produced by FastQC. Quality metrics were observed and all libraries were of high quality. No poor quality sequences, sequence duplication, overrepresented sequences or adapter content was observed. Libraries of WENRC and ENRI pools were aligned to *Mus musculus* reference genome assembly (NCBI37/mm9) with Bowtie2 [5]. To identify H3K27me3 histone modification in the WENRC and ENRI sets the HOMER program suite was utilized [3]. G+C-content was measured with HOMER using the command "makeTagDirectory" with "-checkGC" option. This provides GC% for normalized genomic and tag fractions and can be plotted to visualize the possible G+C-content bias between the genome and sample. No G+C-content bias was observed in the ChIP-Seq samples (Supplemental materials and methods Figure 1). Average sample fragment GC% was within 1.6% of average expected GC% in all samples and input (Supplemental materials and methods table I).

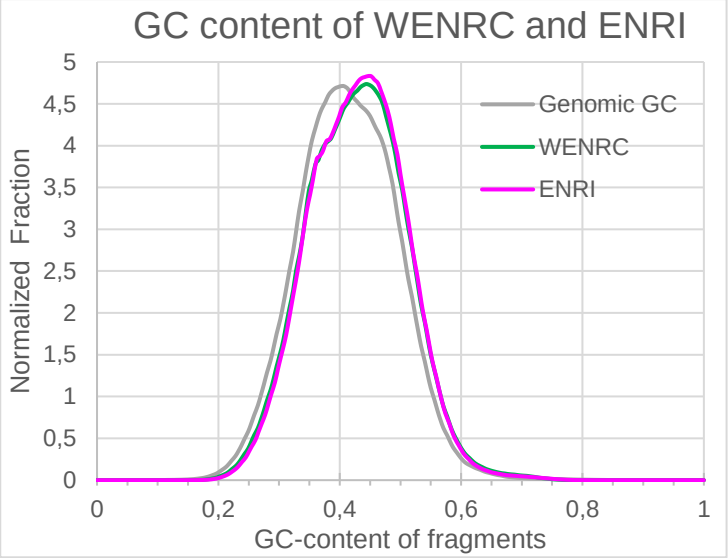

Supplemental materials and methods Figure 1. G+C-content analysis

Supplemental materials and methods table I: GC content in sequenced samples

Sample	Average Fragment GC%	Average Expected GC%
WENRC input	40.96%	41.39%
WENRC	42.82%	41.39%
ENRI input	40.71%	41.40%
ENRI	42.97%	41.39%

Peaks were called with “findPeaks” with parameter “-histone”. This makes the program to identify 500 bp peaks that are significantly enriched compared to input control (4 fold). Variable length peaks are produced by stitching called peaks together if they are within 1000 bp of each other.

Additionally a second round of peak calling for detection of broader peaks was performed with “findPeaks” with parameters “-size 1000” and “-minDist 10000”. Identification of peaks starting with size 1000 bp and stitching range of 10 000 bp allowed the identification of larger histone modification areas.

Regions identified by these approaches were merged. Differentially bound regions were identified with “getDifferentialPeaks” with parameters “-F 2” using previously identified WENRC peaks as targets and

ENRI sample background and vice versa. Two fold (log_2) differences between WENRC and ENRI samples were considered significant when $P < 10^{-12}$ and. This resulted in two list of genes enriched for H3K27me3 in WENRC or ENRI samples.

Identification of intestinal PRC2 targets

Differentially transcribed genes were identified with GRO-Seq and PRC2 targets by H3K27me3 ChIP-Seq as explained above. Altogether, 52 protein coding genes were found repressed by PRC2 in crypts/ISCs (WENRC) and upregulated in enterocytes (ENRI) and 38 genes repressed by PRC2 in enterocytes (ENRI) and upregulated in crypts/ISCs (WENRC) (Figure 2B).

Heatmaps

Differentially expressed transcripts and differentially H3K27me3 modified genes were hierarchically clustered with Cluster 3.0 [6] using average linkage and was visualized in Java Treeview 1.1.6r4 [7]. Read coverage visualizations of H3K27me3 in WENRC and ENRI pools were generated with the deepTools program package by bamCoverage, computeMatrix and heatmapper [8]. File conversion to BAM format was performed using SAMtools [9]. Bigwig files were generated by bamCoverage with binSize 10 and normalized to 1 x sequencing depth using fragment size available from HOMER's Tag directory analysis. Matrixfiles needed for generating the heatmaps were done with the program computeMatrix using TSS as a reference-point with range of ± 10 000 bases. Then the program heatmapper was utilized to retrieve the visualized representation of the H3K27me3 data as a heatmap with a histrogram.

CpG islands

All CpG island locations within the mm9 reference genome were downloaded from the UCSC Genome Bioinformatics Site's Table Browser http://genome.ucsc.edu/cgi-bin/hgTables. CpG island intersections with exact H3K27me3 peaks or -15 kb from TSS of differentially transcribed genes were analyzed with intersectBed from the bedtools suite [10].

Homer de novo motif analyses for intestinal PRC2 target genes

HOMER was utilized to search for enriched motifs with lengths of 6 to 16 bases spanning the TSS from -1000 to +500 bases in H3K27me3 target genes using the differentially expressed, non-PRC2 targets genes as a background.

Intestinal PRC2 targets in colorectal cancers and adenomas

Microarray data for colorectal cancer tumors (GDS4382) [11] and colorectal adenoma formation (GDS2947) [12] were downloaded from http://www.ncbi.nlm.nih.gov/geo/. Two tailed paired Student's t-test with adjusted $P < 10^{-3}$ (Benjamini & Hochberg corrected) was used to determine differently expressed genes in the microarray sets. First, list of genes (n=38) expressed in crypt/ISCs and silenced by PRC2 in enterocytes were compared to genes upregulated in colorectal cancer tumors and adenomas compared to adjacent healthy foci. In these comparisons, from the 38 queried genes, 17 were found upregulated in colon cancers (hypergeometric test: *P < 2.76e-05*) and 18 in adenomas (hypergeometric test: *P < 5.44e-04*) and genes upregulated in both diseases (n=14) are shown in Figures 5B and 5D. Second, list of genes (n=52) expressed in enterocytes and silenced by PRC2 in crypts/ISCs were compared to genes downregulated in colorectal cancer tumors and adenomas compared to adjacent healthy foci. In these comparisons, from the 52 queried genes, 15 were found downregulated in colon cancers (hypergeometric test: *P < 5.15e-03*) and 21 in adenomas (hypergeometric test: *P < 3.17e-03*) and genes upregulated in both diseases (n=12) are shown in figures 5C and 5E.

Gene ontology and pathway analyses

Over-represented gene ontologies and pathways amongst PRC2 targets in crypts/ISCs and enterocytes were analyzed separately in ConsensusPathDB-mouse interaction database (http://cpdb.molgen.mpg.de/MCPDB) [13].

Supplemental materials and methods Table I. List of qRT-PCR oligos used in this study

Oligonucleotide	Species	Sequence (5' to 3')
Gapdh_fwd	*Hs*	TCCATGACAACTTTGGTATCGTGG
Gapdh_rev	*Hs*	GACGCCTGCTTCACCACCTTCT
Lgr5_fwd	*Hs*	GAAGATTTCCTGCTTGACTTTG
Lgr5_rev	*Hs*	GGATCTGAAAACTGTTGAAGTCAC
Alpi_fwd	*Hs*	CCTTTGGTGGCTACACCTTGC
Alpi_rev	*Hs*	CGCCTGCTGCTGGTAATCG
Lyz_fwd	*Hs*	GAGAGTGGTTACAACACACGAGC
Lyz_rev	*Hs*	ATCACGGACAACCCTCTTTGC
Chga_fwd	*Hs*	CTCCAGGTCCGAGGCTACC
Chga_rev	*Hs*	GTAGTGCCTGCAGCTGGTGG
Muc2_fwd	*Hs*	CTGTAAGAAGTGTGAACAGACGC
Muc2_rev	*Hs*	AATGCTGGCATCAAAGTTGG
Gapdh_fwd	*Mm*	TGTGTCCGTCGTGGATCTGA
Gapdh_rev	*Mm*	CCTGCTTCACCACCTTCTTGA
Lgr5_fwd	*Mm*	GACAATGCTCTCACAGACGTCC
Lgr5_rev	*Mm*	CAGGGAGTGGATTCTATTATTATGGAG
Alpi_fwd	*Mm*	CCACAAGGCTTCTACCTCTTTGTAG
Alpi_rev	*Mm*	CGGGTGTAGGATTTGTCATCTAGG
Lyz_fwd	*Mm*	GGAATGGATGGCTACCGTGG
Lyz_rev	*Mm*	CACAGGCATTCTTAGATCTTGGG
Chga_fwd	*Mm*	GTGCGTCCTGGAAGTCATCTCC
Chga_rev	*Mm*	GAGAGCCAGGTCTTGAAGTTCC
Muc2_fwd	*Mm*	GGAACCGGGAAGATGCACTC
Muc2_rev	*Mm*	GTCAGCAGCCTCTCACATTCG
Suz12_fwd	*Mm*	GATGAGAAAGATCCAGAATGGC
Suz12_rev	*Mm*	ATAATTTTCTACAAACAGCATACAGGC
Ezh2_fwd	*Mm*	GTCTGATGTGGCAGGCTGG
Ezh2_rev	*Mm*	GCCCTTTCGGGTTGCATC
Gata4_fwd	*Mm*	GAGCCTGTATGTAATGCCTGCG
Gata4_rev	*Mm*	GGAGGGTCTCACCAGCAGG
Zfp503_fwd	*Mm*	GCACCCAGAGTATTTGCAACCC
Zfp503_rev	*Mm*	CCCTATCTGCGAACATGTTTGAGC
Marcksl1_fwd	*Mm*	GAGGAGGCAGCGGGCGC
Marcksl1_rev	*Mm*	GGCTCGATGGCATCACCAGTAG
Cdk6_fwd	*Mm*	CCTGGAGACCTTCGAGCAC
Cdk6_rev	*Mm*	GTGAGAATGAAGAAAGTCCAGACC
Etv4_fwd	*Mm*	GCGGATACTTGGACCAGCGAG
Etv4_rev	*Mm*	GTCTCTTGGAAGTGACTGAGGTCC
Scin_fwd	*Mm*	CAGCTGGGAGAGCTTCAACAAG
Scin_rev	*Mm*	GACGCTCATATTTGTTGCAGGAG
Arg2_fwd	*Mm*	CAACCAGGAACTGGCTGAAG
Arg2_rev	*Mm*	GGCGTGACCGATAATGGTAC
Sphk1_fwd	*Mm*	CCTGGAGGAGGCAGAGATAACC
Sphk1_rev	*Mm*	CCAGTCTGGCCGTTCCATTAG
Slc15a1_fwd	*Mm*	GATCGCAGACTCGTGGCTGG

Slc15a1_rev	*Mm*	GGAAGGCTGTCAGGACTGCC

Supplemental References

1. Andrews S, Lindebaum P, Howard B, et al. FastQC: a quality control tool for high throughput sequence data. 2010.

2. Langmead B, Trapnell C, Pop M, et al. Ultrafast and memory-efficient alignment of short DNA sequences to the human genome. Genome Biol 2009:1–10.

3. Heinz S, Benner C, Spann N, et al. Simple Combinations of Lineage-Determining Transcription Factors Prime cis-Regulatory Elements Required for Macrophage and B Cell Identities. Mol. Cell 2010;38(4):576–589.

4. Robinson MD, McCarthy DJ, Smyth GK. edgeR: a Bioconductor package for differential expression analysis of digital gene expression data. Bioinformatics 2010;26(1):139–40.

5. Langmead B, Salzberg SL. Fast gapped-read alignment with Bowtie 2. Nat. Methods 2012;9(4):357–9.

6. Hoon MJL de, Imoto S, Nolan J, et al. Open source clustering software. Bioinformatics 2004;20(9):1453–1454.

7. Saldanha AJ. Java Treeview–extensible visualization of microarray data. Bioinformatics 2004;20(17):3246–8.

8. Ramírez F, Dündar F, Diehl S, et al. DeepTools: A flexible platform for exploring deep-sequencing data. Nucleic Acids Res. 2014;42(W1).

9. Li H, Handsaker B, Wysoker A, et al. The Sequence Alignment/Map format and SAMtools. Bioinformatics 2009;25(16):2078–2079.

10. Quinlan AR, Hall IM. BEDTools: A flexible suite of utilities for comparing genomic features. Bioinformatics 2010;26(6):841–842.

11. Khamas A, Ishikawa T, Shimokawa K, et al. Screening for epigenetically masked genes in colorectal cancer using 5-aza-2`-deoxycytidine, microarray and gene expression profile. Cancer Genomics and Proteomics 2012;9(2):67–75.

12. Sabates-Bellver J, Flier LG Van der, Palo M de, et al. Transcriptome profile of human colorectal adenomas. Mol. Cancer Res. 2007;5(12):1263–1275.

13. Kamburov A, Stelzl U, Lehrach H, et al. The ConsensusPathDB interaction database: 2013 Update. Nucleic Acids Res. 2013;41(D1).

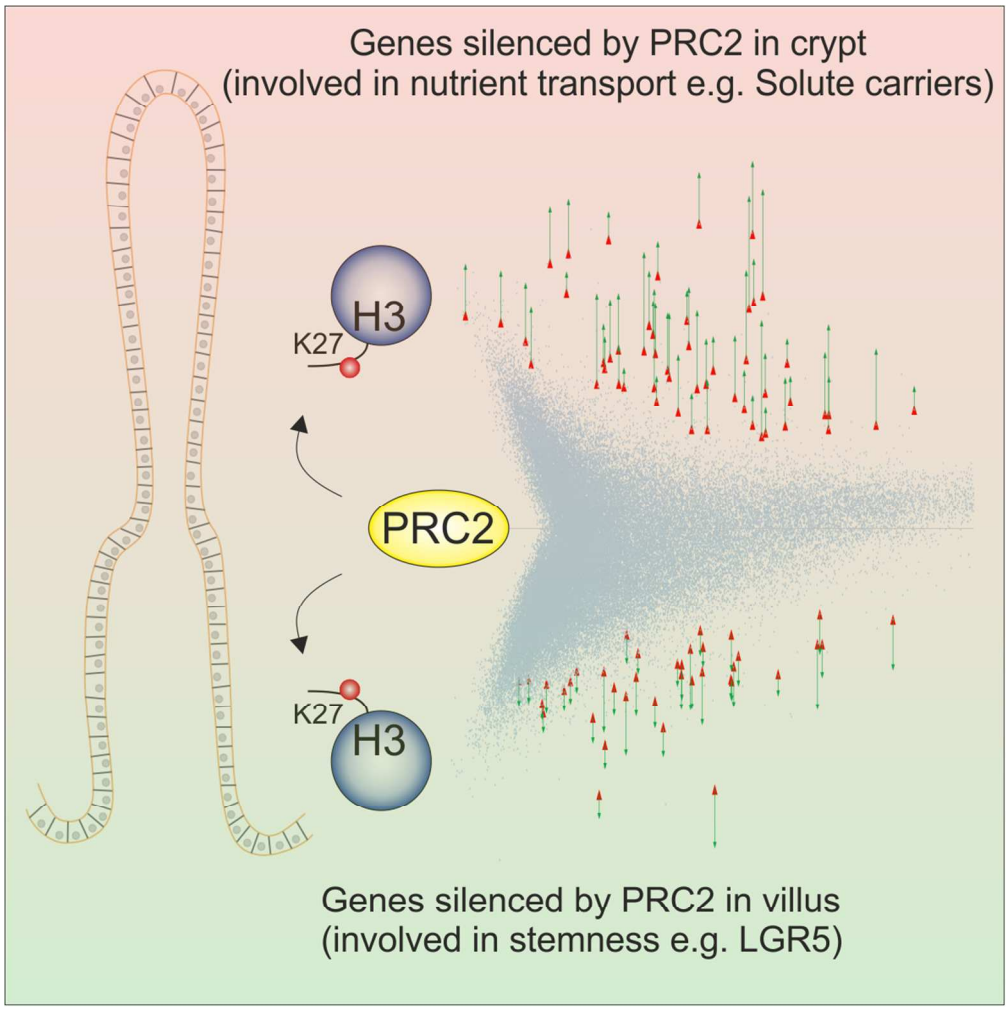

100x100mm (300 x 300 DPI)